RSC Advances

PAPER

View Article Online
View Journal | View Issue

Cite this: *RSC Adv.*, 2015, **5**, 33838

Sequential palladium catalyzed coupling–cyclocondensation–coupling (C^3) four-component synthesis of intensively blue luminescent biarylsubstituted pyrazoles†

Melanie Denißen,[a] Jan Nordmann,[a] Julian Dziambor,[a] Bernhard Mayer,[a] Walter Frank[b] and Thomas J. J. Müller*[a]

Received 18th February 2015
Accepted 30th March 2015

DOI: 10.1039/c5ra03104d

www.rsc.org/advances

1-, 3-, and 5-Biarylsubstituted pyrazoles can be efficiently prepared by a microwave-assisted consecutive four-component synthesis based upon a sequential Pd-catalyzed coupling–condensation–coupling (C^3), a one-pot sequence which concatenates Sonogashira alkynylation and Suzuki arylation intercepted by pyrazole forming cyclocondensation of the ynone intermediate. This diversity-oriented approach enables tailoring, fine-tuning and optimization of absorption and emission properties towards high fluorescence quantum yields in solution up to $\Phi_f = 0.97$. The increased luminescence intensity stemming from biaryl substitution can be rationalized by ground and excited state computations on the DFT level of theory, which nicely reproduce the experimental data of absorption and emission.

Introduction

Pyrazoles are omnipresent in many fields of science and technology. Although they are rarely found in nature,[1] they have applications as pesticides in crop protection[2] and their biological activities encompass analgesic, anti-inflammatory, sedative, antipyretic, and antispasmodic activity.[3] In addition, these heterocycles are known as pluripotent ligands[4] in coordination chemistry. Furthermore, pyrazoles have also aroused interest due their photophysical properties and applications such as optical brighteners as additives in detergents,[5] UV-stabilizer for polystyrene,[6] and highly selective fluorescence sensors.[7] Quite some derivatives display large Stokes shifts and emission at short wavelength, *i.e.* blue luminescence, which remains an ongoing challenge in OLED technologies.[8] Hence, novel syntheses of pyrazoles are highly attractive evergreens for organic chemists.

The interesting photophysical properties of pyrazoles as fluorophores and the challenge to access tailor-made π-systems by diversity-oriented syntheses (DOS)[9] such as multicomponent reactions (MCR) have prompted us to develop a regioselective consecutive three-component Sonogashira coupling–cyclocondensation (C^2) synthesis of 1,3,5-substitued pyrazoles in a one-pot fashion (Scheme 1).[10] All 1,3,5-substituted pyrazoles are highly fluorescent dyes with large Stokes shifts and moderate quantum yields.

It is known that biphenyl is essentially coplanar in the first excited state S_1, while the phenyl rings are distorted from coplanarity by ~44° in the electronic ground state S_0.[11,12] This peculiar aspect was successfully considered for designing fluorescent chemosensors.[13] For increasing fluorescence quantum yields we envisioned the implementation of extended delocalization by employing a DOS approach to biaryl pyrazoles. Therefore, biaryl substitution on the pyrazole core in 1-, 3-, and 5-position (Fig. 1) could guide the way for combining the photophysical characteristics of biaryls with pyrazole based emitters supported by systematic quantitative structure–activity relationship (QSAR) studies.

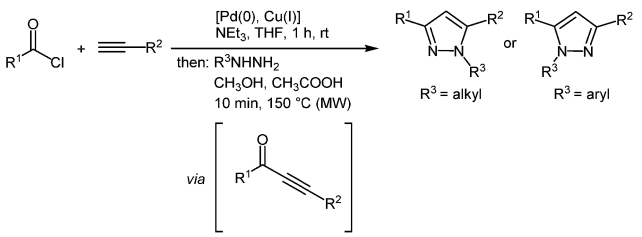

Scheme 1 Regioselective coupling–cyclocondensation (C^2) synthesis of 1,3,5-substituted pyrazoles.

[a]*Institut für Organische Chemie und Makromolekulare Chemie, Heinrich-Heine-Universität Düsseldorf, Universitätsstraße 1, 40225 Düsseldorf, Germany. E-mail: ThomasJJ.Mueller@uni-duesseldorf.de*

[b]*Institut für Anorganische Chemie und Strukturchemie, Heinrich-Heine-Universität Düsseldorf, Universitätsstraße 1, 40225 Düsseldorf, Germany*

† Electronic supplementary information (ESI) available: Synthesis of reference compound **9**, ^{1}H and ^{13}C NMR spectra, UV/Vis and fluorescence spectra of compounds **5**, **6**, **7**, **8**, and **9**; computed *xyz*-coordinates of the S_0 state of the pyrazoles **5c**, **6d**, and **8b**, computed UV/Vis spectra of TD-DFT calculated structures of **5c**, **6d**, and **8b**, computed xyz-coordinates of the S_1 state of pyrazole **6d**. CCDC 1049137. For ESI and crystallographic data in CIF or other electronic format see DOI: 10.1039/c5ra03104d

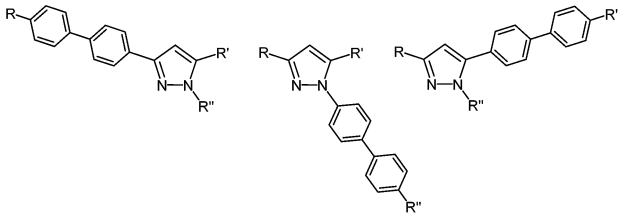

Fig. 1 Biaryl substitution pattern of 1,3,5-substituted pyrazoles.

Modular, flexible and reactivity-based procedures are currently highly topical methodologies in one-pot syntheses of heterocycles.[14] Conceptually, instead of applying biaryl starting materials to the ynone strategy we considered a DOS approach based upon sequential catalysis.[15] In the sense of a self-relay catalysis[16] the initially employed catalyst source should catalyze a subsequent catalytic step without further addition of the metal complexes. As a consequence a straightforward one-pot process furnishing diversely functionalized molecules can be envisioned. In addition, the combined advantages of MCR and sequential catalysis enhance the synthetic and catalytic efficiency and efficacy.[17] In this context sequential Pd-catalyzed processes[15] should pave the way to expanded pyrazoles in the sense of *de novo* generation-functionalization of the pyrazole core. Therefore, the concatenation of the C^2 sequence with a concluding Suzuki–Miyaura coupling in a one-pot fashion promises a highly modular access to intensely fluorescent biarylsubstituted pyrazoles (Scheme 2).

Here, we report a novel sequentially Pd-catalyzed C^3-synthesis of biarylsubstituted pyrazoles in a consecutive four-component fashion. In addition, the photophysical properties in solution are reported and discussed in the light of DFT-computational studies.

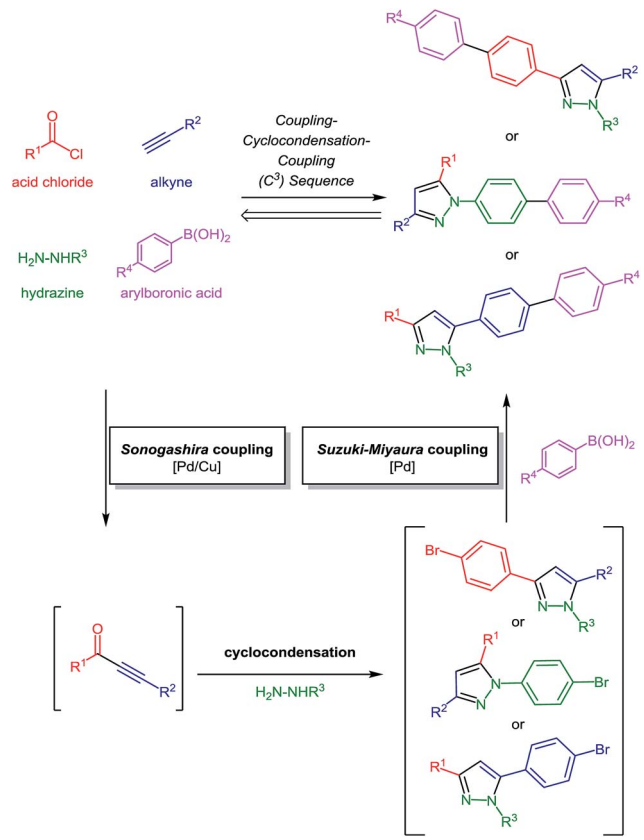

Scheme 2 Retrosynthetic analysis of biarylsubstituted substituted pyrazoles *via* coupling–condensation–coupling (C^3) one-pot transforms.

Results and discussion

Synthesis

For establishing the sequentially Pd(0)-catalyzed microwave-assisted C^3-four-component synthesis of 1,3,5-substituted pyrazoles containing biaryl units we first set out to place the dormant bromine functionality in the alkynyl part. Based upon previous studies on one-pot sequences with terminal Suzuki coupling[9b] the addition of 20 mol% of triphenylphosphane is necessary to stabilize the catalytically active Pd(0) species.

Therefore, upon coupling various (hetero)aroyl chlorides **1** with *p*-bromophenyl acetylene (**2a**) the expected alkynones are formed that were subsequently cyclocondensed with hydrazines **3** and then, still within the same reaction vessel and without further addition of metal complexes, different boronic acids **4** were coupled to give the desired 5-biarylsubstituted pyrazoles **5** in moderate to good yields (Scheme 3, Table 1). The structures of the compounds **5** were unambiguously assigned by ^{1}H and ^{13}C NMR spectroscopy and mass spectrometry.

However, these optimized reaction conditions (Scheme 3) cannot be directly transposed to the synthesis of 3-substituted pyrazoles starting from 4-bromo benzoyl chloride (**1d**). The model reaction with acid chloride **1d**, phenyl acetylene (**2b**), methyl hydrazine (**3a**), and phenyl boronic acid (**4b**) in THF gives rise to the formation of the desired 3-substituted pyrazole **6a** only in 26% (2 h for the Sonogashira coupling step) and 39% (17.5 h for the Sonogashira coupling step). However, changing the solvent to 1,4-dioxane considerably improves the overall yield of product **6a** with a Sonogashira coupling time of 2 h.

When applying these conditions to the C^3-four-component sequence of 4-bromo benzoyl chloride (**1d**), alkynes **2**, methyl hydrazine (**3a**), and arylboronic acids **4** 3-biarylsubstituted pyrazoles **6** can be obtained in good yields (Scheme 4, Table 2). The structures of the compounds **6** were unambiguously assigned by ^{1}H and ^{13}C NMR spectroscopy and mass spectrometry.

The substitution pattern of the pyrazole core can be varied by the choice of different alkynes **2** and boronic acids **4**. In addition

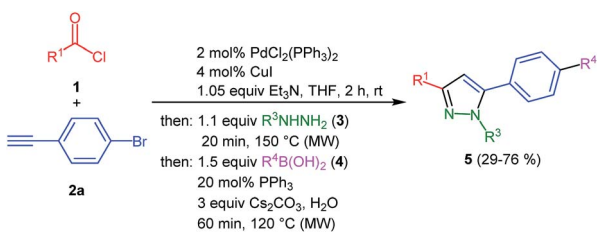

Scheme 3 Consecutive C^3-four-component synthesis of 5-biarylsubstituted pyrazoles **5**.

Table 1 Consecutive C^3-four-component synthesis of 5-biarylsubstituted pyrazoles **5**

Entry	Acid chloride **1**	Hydrazine **3**	Boronic acid **4**	5-Biarylsubstituted pyrazoles **5** (yield)
1	$R^1 = C_6H_5$ (**1a**)	$R^3 = CH_3$ (**3a**)	$R^4 = 4\text{-}MeC_6H_4$ (**4a**)	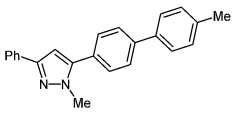 **5a** (67%)
2	**1a**	**3a**	$R^4 = C_6H_5$ (**4b**)	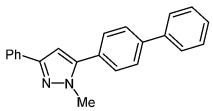 **5b** (76%)
3	**1a**	**3a**	$R^4 = 2\text{-}Me\text{-}4\text{-}FC_6H_3$ (**4c**)	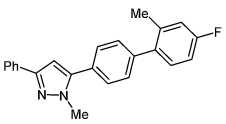 **5c** (66%)
4	$R^1 = 2\text{-}FC_6H_4$ (**1b**)	**3a**	**4a**	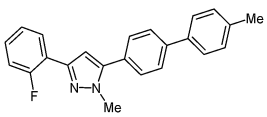 **5d** (29%)
5	R^1 = 2-thienyl (**1c**)	**3a**	**4a**	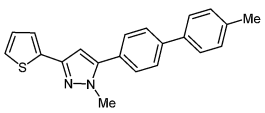 **5e** (68%)
6	**1c**	**3a**	$R^4 = 4\text{-}MeOC_6H_4$ (**4d**)	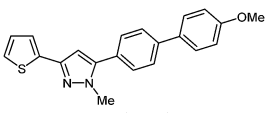 **5f** (43%)
7	**1a**	$R^3 = H$ (**3b**)[a]	**4a**	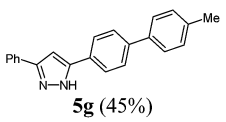 **5g** (45%)

[a] Employed as $N_2H_4 \cdot H_2O$.

to aryl substituents a butyl substituent can be uneventfully introduced in the 5-position (Table 2, entry 3). Electron neutral and electron withdrawing aryl boronic acids (Table 2, entry 4) are well tolerated in the reaction sequence. Sterically hindered boronic acids can also be coupled (Table 2, entry 2).

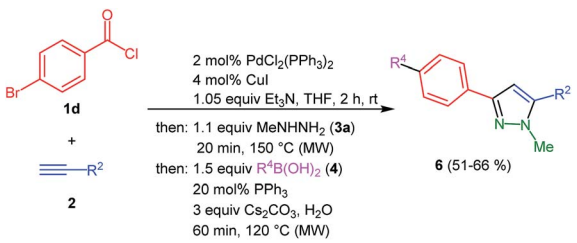

Scheme 4 Consecutive C^3-four-component synthesis of 3-biarylsubstituted pyrazoles **6**.

In the sense of a consecutive C^3-pseudo-five-component synthesis starting from 4-bromo benzoyl chloride (**1d**), *p*-bromophenyl acetylene (**2a**), methyl hydrazine (**3a**), and phenyl boronic acid (**4b**) the 3,5-bis(biphenyl) 1-methyl pyrazole (**7**) was obtained in 37% yield, *i.e.* an average yield of 72% per step in this three-step one-pot process (Scheme 5). The structure of compound **7** was unambiguously assigned by ^1H and ^{13}C NMR spectroscopy and mass spectrometry.

Finally, we also planned to couple a bromophenyl substituent in the 1-position. However, the standard conditions for the synthesis of 3- and 5-biphenylic substituted pyrazoles **5** and **6** were found to be unsuitable for accessing this substitution pattern. The problem already arose in the pyrazole formation step. Careful optimization of these first two steps revealed dichloromethane as a solvent with a reaction time of 16 h at room temperature for the Sonogashira step and subsequent cyclocondensation with dielectric heating at 100 °C for 40 min

Table 2 Consecutive C^3-four-component synthesis 3-biarylsubstituted pyrazoles **6**

Entry	Alkyne **2**	Boronic acid **4**	3-Biarylsubstituted pyrazoles **6** (yield)
1	$R^2 = C_6H_5$ (**2b**)	**4b**	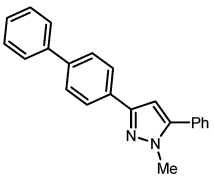 **6a** (66%)
2	$R^2 = 4\text{-}MeC_6H_4$ (**2c**)	**4c**	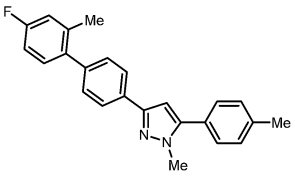 **6b** (51%)
3	$R^2 = n\text{-}C_4H_9$ (**2d**)	**4b**	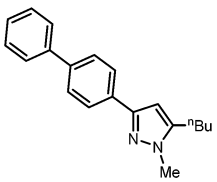 **6c** (61%)
4	**2b**	$R^4 = 4\text{-}NCC_6H_5$ (**4e**)	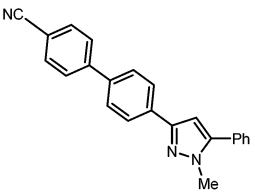 **6d** (59%)

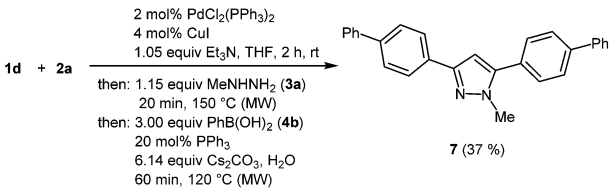

Scheme 5 Consecutive C^3-pseudo-five-component synthesis of 3,5-bis(biphenyl) 1-methyl pyrazole (**7**).

gave 1-*p*-bromophenyl-3,5-diphenylpyrazole in 61% yield. These modifications were then employed in the consecutive four-component synthesis to give 1-biarylsubstituted pyrazoles **8** in moderate to good yields (Scheme 6, Table 3). The structures of the compounds **8** were unambiguously assigned by ^1H and ^{13}C NMR spectroscopy and mass spectrometry, and later by an X-ray crystal structure analysis of compound **8b** (Fig. 2). Although, in the cases of the pyrazoles **5**, **6**, and **7** exclusively the regioisomers arising from the Michael addition of the inner nitrogen atom of the hydrazines were formed, the regioselectivity for aryl hydrazines was inverted giving preferentially the products arising from the Michael addition of the outer nitrogen atom. For compounds **8e–h** the minor regioisomer could be identified and quantified by ^1H NMR spectroscopy. The regioselectivity in these cases lies between 6 : 1 and 22 : 1 in favor of the depicted regioisomers.

This sequence also allows the use of boronic acid esters (Table 3, entry 4) besides the usually employed boronic acids without changing the reaction conditions. Besides structural elucidation by spectroscopy the solid state structure of the pyrazole **8b** was additionally corroborated by single crystal X-ray analysis (Fig. 2).[18]

The X-ray diffractional and DFT-computed (upon employing a solvent model, *vide infra*) torsional angles of the phenyl substituents are in good agreement (Table 4). In contrast to the optimized calculated solution geometry only for the phenyl substituent in position 3 of the pyrazole core the crystal

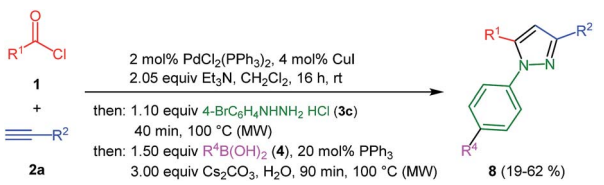

Scheme 6 Consecutive C^3-four-component synthesis of 1-biaryl-substituted pyrazoles **8**.

Table 3 Consecutive C^3-four-component synthesis of 1-biarylsubstituted pyrazoles **8**

Entry	Acid chloride **1**	Alkyne **2**	Boronic acid **4**	1-Biarylsubstituted pyrazoles **8** (yield)
1	**1a**	**2b**	**4b**	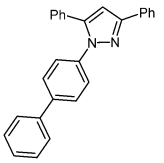 **8a** (57%)
2	**1a**	**2b**	**4a**	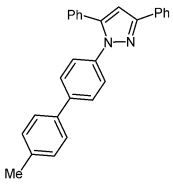 **8b** (59%)
3	**1a**	**2b**	**4e**	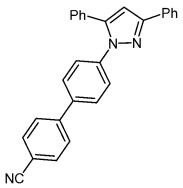 **8c** (62%)
4	**1a**	**2b**	2-Bpin-5-methyl-thio-phene (**4f**)	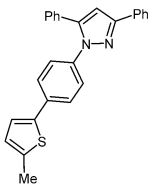 **8d** (55%)
5	$R^1 = 4\text{-}MeOC_6H_4$ (**1e**)	**2b**	**4a**	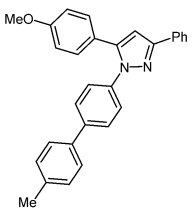 **8e** (44%, rr 14:1)[a]
6	$R^1 = 2\text{-}ClC_6H_4$ (**1f**)	**2b**	**4a**	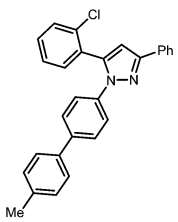 **8f** (19%, rr 10:1)[a]
7	**1c**	**2b**	**4a**	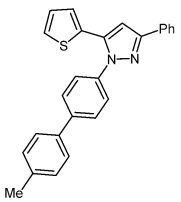 **8g** (55%, rr 22:1)[a]

Table 3 (*Contd.*)

Entry	Acid chloride **1**	Alkyne **2**	Boronic acid **4**	1-Biarylsubstituted pyrazoles **8** (yield)
8	**1a**	**2d**	**4a**	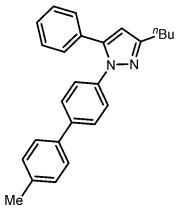 **8h** (60%, rr 6:1)[a]

[a] The ratio of regioisomers, rr, was determined by intergration of the characteristic proton signal of the methine group.

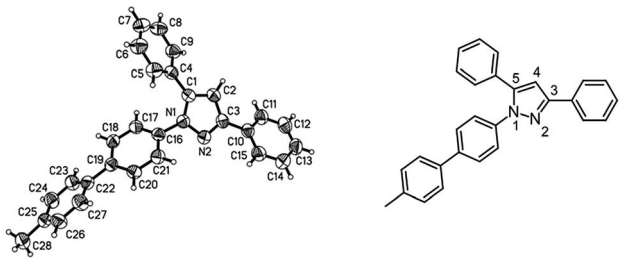

Fig. 2 Diagram of the structure of the molecules of compound **8b** in the crystal; 30% probability ellipsoids (enumeration of the pyrazole core on the left).

structure reveals a considerable twist out of coplanarity, which can be most likely attributed to crystal packing of compound **8b**.

The crystal packing of the molecules of pyrazole **8b** reveals an acentric structure (space group $Pca2_1$) (Fig. 3). The sheer number of π-systems suggests many intermolecular π–π-interactions to be present in the solid. However, only van der Waals interactions can be observed. A closer inspection reveals van der Waals interactions of one distinct molecule to entirely ten nearest neighbors which cannot be specified in more detail here. As a special feature only a coordinated multiple T-shape interaction can be found (Fig. 4).

Photophysical properties and calculated electronic structure

All solutions of the synthesized biarylsubstituted pyrazoles **5–8** show a remarkable blue fluorescence in solution upon eyesight. Therefore, the photophysical properties were determined by UV/Vis and static fluorescence spectroscopy (Table 5). For comparison to simple arylsubstituted pyrazoles we prepared 1-methyl-3,5-diphenylpyrazole (**9**) according to our previously published protocol (for experimental details see ESI†).[10a] The longest wavelength absorption maxima $\lambda_{max,abs}$ of the 3- and 5-biarylsubstituted pyrazoles **5–7** are found in a broad range from 263.0 to 306.5 nm with a molar extinction coefficients ε between 33 000 to 44 000 L cm^{-1} mol^{-1}. As a consequence of the large extended π-electron conjugation the 3,5-bis(biphenyl) substituted pyrazole **7** display a particularly high molar extinction coefficient ε of 62 500 L cm^{-1} mol^{-1}. The absorption maxima of the 1-aryl substituted compounds **8** ranges between 256.5 and 311.0 nm with molar extinction coefficients ε of 18 900 to 39 900 L cm^{-1} mol^{-1}. In general the high molar extinction coefficients ε can be ascribed to the dominance of π–π* transitions. The absorption maximum of the simple pyrazole **9** is hypsochromically shifted in comparison to the consanguineous biarylsubstituted pyrazoles **5b**, **6a**, and **7** as a consequence of the extended π-system by biaryl substitution. The absorption maximum of **9** could be detected at 254.0 nm with a molar extinction coefficient of 28 800 L cm^{-1} mol^{-1}. The transition at highest energy of pyrazole **8a** (257.0 nm) can be assigned to the absorption of the pyrazole core as in the case of the simple pyrazole **9**.

For the emission maxima $\lambda_{max,em}$ 3- and 5-biarylsubstituted pyrazoles **5–7** span a wider range ($\lambda_{max,em}$ 338.5–394.0 nm) than the 1-biarylsubstituted pyrazoles **8** ($\lambda_{max,em}$ 382.5–394.0 nm). In

Table 4 Measured and computed torsional angles of the phenyl rings in pyrazole **8b**

	Torsion angels [°]	
	$\theta_{X\text{-ray}}$	$\theta_{calc.}$
N(1)–C(1)–C(4)–C(5)	35.0(3)	45
N(2)–C(3)–C(10)–C(15)	−26.1(3)	4
N(2)–N(1)–C(16)–C(21)	44.8(2)	48
C(20)–C(19)–C(22)–C(27)	26.3(2)	37

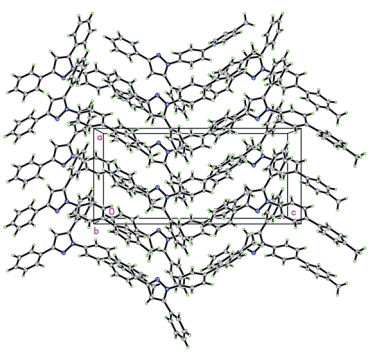

Fig. 3 Crystal packing diagram of compound **8b** displaying the orthorhombic unit cell.

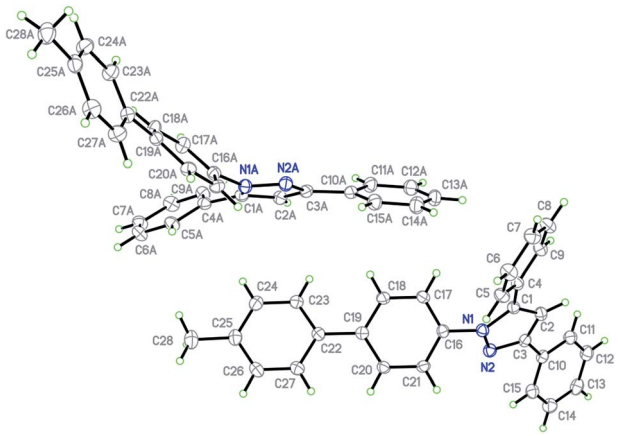

Fig. 4 Coordinated multiple T-shape interaction in the crystal of compound **8b**.

comparison the diphenyl derivative **9** possesses an emission maximum at 338.5 nm. The observed large Stokes shift of 9800 cm^{-1} arises from the well-established pronounced conformational change in the pyrazole core upon excitation.[19] While the relative fluorescence quantum yields Φ_f of 3- and 5-biarylsubstituted pyrazoles **5–7** are with the exceptions of compounds **6d** and **7** generally high (Φ_f = 0.27–0.97), 1-aryl substituted compounds **8** lie with Φ_f = 0.12–0.41 generally lower. Moreover, in comparison of the simple pyrazole **9** (Φ_f = 0.40) with the consanguineous series pyrazoles **5b**, **6a**, and **8a** as well as **7** the fluorescence quantum yields of **5b** (Φ_f = 0.77) and **6a** (Φ_f = 0.49) have increased, it remains identical for **8a** (Φ_f = 0.41), however, strongly decreases for the bis(biphenyl) compound **7** (Φ_f = 0.07).

For all substitution patterns the Stokes shifts $\Delta\tilde{\nu}$ are very pronounced and are found between 6000 and 11 300 cm^{-1}. The occurrence of large Stokes shifts can be generally attributed to two mechanistic pathways based on the excited state properties of the molecules. Either the geometry of the molecule changes considerably in the excited state or a reorganization of solvent molecules after excitation becomes responsible.[19] This latter solvent effect increases for molecules with larger excited state dipole moments than in their ground state.[20] 3,5-Diarylsubstituted pyrazoles are known for their strongly polar nature in the excited state.[6] For 3- and 5-biarylsubstituted pyrazoles **5–7** one distinct maximum can be detected in the absorption spectra (Fig. 5 and 6). However 1-biarylsubstituted pyrazoles **8** often show an additional characteristic shoulder around 300 nm (Fig. 5). The direct comparison of the absorption and emission properties of the regioisomers **5b** and **6a** reveals significant differences (Fig. 6). While the absorption maximum of compound **6a** is shifted bathochromically in comparison to pyrazole **5b** by 2000 cm^{-1} the emission maximum appears with a hypsochromic shift of 1200 cm^{-1}. So, this shift causes a smaller Stokes shift. This shift of **5b** can be rationalized by planarization of the biphenyl unit in the excited state.

The substituent effects on the fluorescence quantum yields are quite substantial. While cyano substitution (compounds **6d** and **8c**) causes a significant decrease of Φ_f, a similar, yet smaller tendency due to additional rotational degrees of freedom[23] can be observed for *n*-butyl substituted pyrazoles **6c** and **8h**, and pyrazoles with a thienyl substituent in a remote position as in compound **8d** or in 5-position (compound **8g**). For the two sanguineous 3-thienyl pyrazoles **5e** and **5f** the remote *para*-substituent of the biaryl moiety exerts a distinct difference.

Table 5 Selected photophysical properties of biarylsubstituted pyrazoles **5–8** and 1-methyl-3,5-diphenylpyrazole (**9**) at room temperature

Compound	Absorption maxima $\lambda_{max,abs}$ (ε)[a] [nm] (L cm^{-1} mol^{-1})	Emission maxima $\lambda_{max,em}$ (Φ_f)[b] [nm] (a.u.)	Stokes-shift $\Delta\tilde{\nu}$[c] [cm^{-1}]
5a	273.5 (40 100)	357.0 (0.77)	9400
5b	268.5 (36 700)	359.0 (0.77)	8600
5c	263.0 (38 400)	344.5 (0.67)	9000
5d	281.0 (34 200)	351.5 (0.97)	7100
5e	285.0 (44 000)	382.0 (0.35)	8900
5f	289.0 (43 300)	363.0 (0.80)	7100
5g	285.0 (42 000)	343.5 (0.86)	6000
6a	283.5 (35 600)	344.5 (0.49)	6300
6b	267.5 (35 800)	338.5 (0.83)	7800
6c	286.0 (33 000)	347.0 (0.27)	6200
6d	306.5 (36 600)	384.0 (0.10)	6600
7	288.5 (62 500)	367.0 (0.07)	7400
8a	257.0 (36 300), 293.0 sh (25 000)	385.0 (0.41)	8200
8b	257.0 (32 000), 296.0 sh (23 000)	388.0 (0.33)	8000
8c	257.0 (27 400), 307.5 (18 900)	387.0 (0.12)	6700
8d	268.5 (29 500)	385.0 (0.29)	11 300
8e	261.5 (39 900), 288.0 sh (29 600), 311.0 sh (20 500)	386.5 (0.37)	6300
8f	256.5 (27 260), 296.0 (28 404)	388.5 (0.35)	8000
8g	272.5 (39 600)	394.0 (0.30)	11 300
8h	286.0 (22 900)	382.5 (0.33)	8800
9	254.0 (28 800)	338.5 (0.40)	9800

[a] Recorded in CH_2Cl_2 UVASOL (in the absorption maxima sh stands for shoulder). [b] Recorded in CH_2Cl_2 UVASOL. Quantum yields Φ_f were determined with *p*-terphenyl as a standard in cyclohexane UVASOL, Φ = 0.89.[21,22] [c] $\Delta\tilde{\nu} = \lambda_{max,abs} - \lambda_{max,em}$ [cm^{-1}].

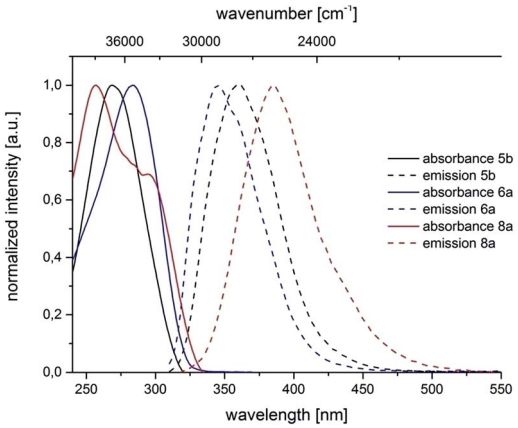

Fig. 5 Selected normalized absorption and emission spectra of biarylsubstituted pyrazoles **5b**, **6a** and **8a** (recorded in CH_2Cl_2 UVASOL at $T = 293$ K, $\lambda_{exc} = 290.0$ nm).

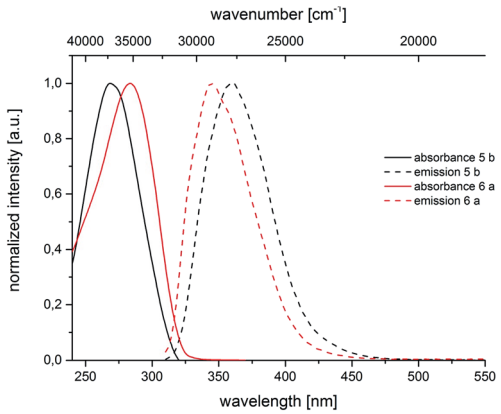

Fig. 6 Normalized absorption and emission spectra of pyrazoles **5b** and **6a** (recorded in CH_2Cl_2 UVASOL at $T = 293$ K, $\lambda_{exc} = 290.0$ nm).

While the methyl substituent only leads to a mediocre quantum yield the methoxy substituent displays a significant magnitude. Interestingly, the 2-phenyl congener **5a** possesses substantially higher fluorescence efficiency than the 2-thienyl derivative **5e**. However, most remarkably are the effects of remote (compounds **5c** and **6b**) and *ortho*-fluorophenyl substitution (compound **5d**) at the position 3 and 5 of the pyrazole core. Indeed the 3-(*ortho*-fluorophenyl) substituted pyrazole **5d** almost reaches unity for the fluorescence efficiency. In summary redshifted emission and highest quantum yields for the solution emission can be obtained upon placing biaryl substituents in the 3- or 5-positions of the pyrazole core.

The observed tunable photophysical behavior of the different series of biarylsubstituted pyrazoles calls for a deeper understanding of the electronic structure, in particular, the nature of relevant longest wavelength transition. Therefore, the geometries of the electronic ground state structures of the pyrazoles **5c**, **6d**, and **8b** were optimized on the DFT level of theory using Gaussian09 (ref. 24) with the B3LYP functional[25] and the Pople 6-311G(d,p) basis set.[26] Since all experimental photophysical data were obtained in dichloromethane

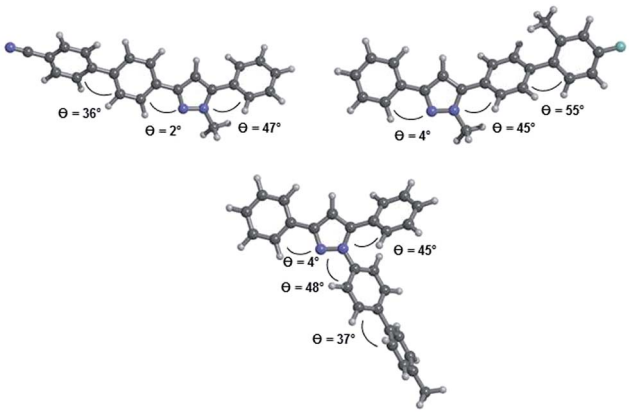

Fig. 7 Optimized geometries at the B3LYP 6-311G(d,p) level of DFT theory for the pyrazole structures **6d** (top left), **5c** (top right), and **8b** (bottom).

solutions the calculations were carried out applying the Polarizable Continuum Model (PCM) with dichloromethane as a solvent.[27] All minimum structures were unambiguously confirmed by analytical frequency analysis.

The inspection of the equilibrium ground state structures for all three different substitution patterns reveals that the torsional angles $\theta_{calc.}$ between the phenyl residues in 3- and 5-position and the adjacent C(1)–N(5) or C(3)–N(4)-atoms only show marginal differences (Fig. 7). Even for the 1-biarylsubstituted pyrazole **8b** the torsional angle remains in the same range. While the 3-phenyl substituents adopt an almost coplanar orientation with the pyrazole core ($\theta_{calc.} = 2$–$4°$) the

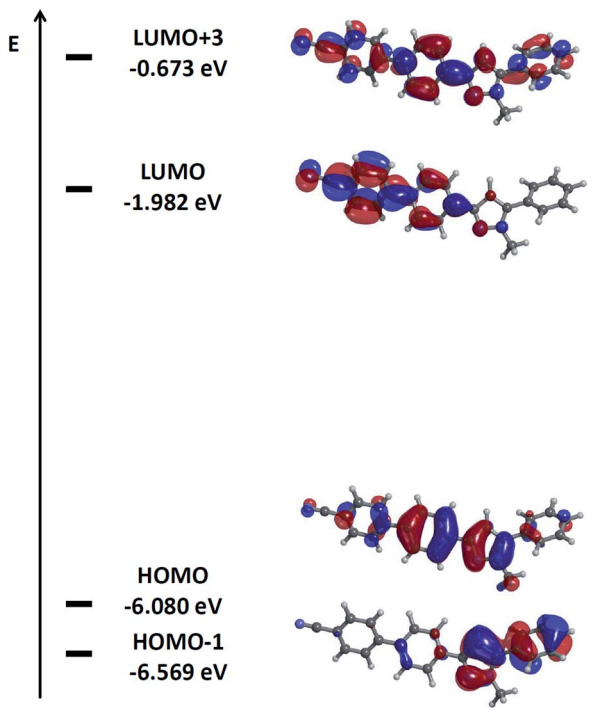

Fig. 8 Selected DFT-computed (B3LYP 6-311G(d,p)) Kohn–Sham frontier molecular orbitals of pyrazole **6d**.

Table 6 TD-DFT calculations (CAM-B3LYP 6-311G(d,p)) of the absorption maxima for the pyrazoles **5c**, **6d** and **8b**

Structure	Experimental $\lambda_{max,abs}$ [nm]	Computed $\lambda_{max,abs}$ [nm] (most dominant contributions)
5c	263	256 (HOMO−1 → LUMO (45%)), (HOMO → LUMO (39%))
6d	307	298 (HOMO → LUMO (86%))
8b	257	243 (HOMO → LUMO +1 (20%))
		245 (HOMO → LUMO +2 (32%))
	296	278 (HOMO → LUMO (85%))

aromatic substituent in 5-position is considerably twisted out of coplanarity ($\theta_{calc.}$ = 45–47°). The ground state equilibrium geometries of the biaryl moieties in all three substituent positions are inherently and expectedly not coplanar[28] and dihedral angles between the two arene rings are found at $\theta_{calc.}$ = 36–37° for **6d** and **8b** and at $\theta_{calc.}$ = 55° for **5c**, the latter as a steric effect of the *ortho*-methyl group. Therefore the electronic communication can be expected to be more efficient biphenyl cores without *ortho*-substitution.

A closer inspection of the coefficient densities in the Kohn–Sham frontier molecular orbitals of pyrazole **6d** reveals that the HOMO's coefficient density is largely localized on the pyrazole core and the 3-aryl substituent (Fig. 8). Furthermore, the remote benzonitrile substituent and the 5-phenyl substituent only bear marginal coefficient density. In contrast, the coefficient density in the LUMO representing cum grano salis the Franck–Condon state upon excitation is almost completely inverted. The major density is now localized on the terminal benzonitrile moiety and its adjacent phenylene fragment, whereas just marginal residual density is found on the pyrazole core and none on the 5-phenyl substituent. Significant coefficient density on the 3-phenylene moiety both in HOMO and LUMO indicates a sufficient overlap between the ground and presumed excited state wavefunctions required for substantial transition dipole moment.

The optimized structures for the pyrazoles **5c**, **6d**, and **8b** were submitted to TD-DFT calculations for assigning the absorption characteristics (Table 6). All calculations were performed for dichloromethane as a solvent. Furthermore, the hybrid exchange-correlation functional CAM-B3LYP[29] was implemented and a non-equilibrium solvation[30] for the state specific solvation of the vertical excitation was included. The computed results are in good agreement with the experimentally determined values. Expectedly, the longest wavelength absorption maxima for the structures **6d** and **8b** appearing around 300 nm result from dominant HOMO → LUMO transitions. The absorption maximum of pyrazole **5c** is shifted hypsochromically due to a considerable torsion by the *ortho*-tolyl substituent. In this case the dominant contribution not only arises from the HOMO → LUMO transition but also from the HOMO−1 → LUMO transition. For 1-biarylsubstituted pyrazoles **8** second maxima are often detected in experimental absorption spectra. For elucidation of this behavior the oscillatory strength of the first ten excited states of **8b** were compared. The inspection reveals that the absorption at lower wavelengths not only consists of one but also of two different excited states, in particular, the excited states S_3 and S_4 are apparently superimposed.

In addition the geometry of the vibrationally relaxed excited state (S_1)[31] of structure **6d** was optimized by a gas phase DFT calculation using the program package Turbomole[32,33] with the B3LYP functional and the TZVP basis set.[34] COSMO (Conductor-like Screening Model)[35] has not been implemented for excited state calculations so far, thus, no solvent model computations were performed. It is also noteworthy to mention that the vibrationally relaxed S_1 state possess a coplanar geometry of the

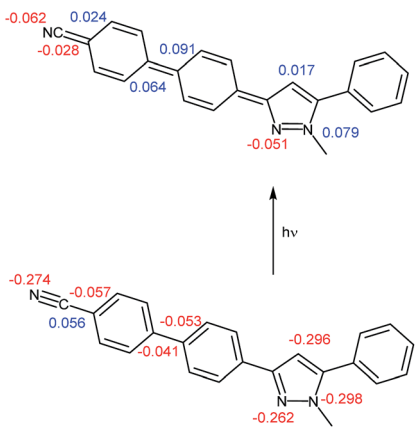

Fig. 9 Non polar ground state (S_0) structure (bottom) and dipolar structure of vibrationally relaxed first excited state (S_1) structure (top) of pyrazole derivative **6d** with partial charges (positive: blue, negative: red).

Table 7 Selected computed bond lengths [Å] for **6d** in the vibrationally relaxed S_0 (Gaussian09/B3LYP/6-311G(d,p)) and S_1 states (Turbomole/B3LYP/def-TZVP)

Bonds	S_0	S_1
C1–C2	1.39	1.37
C1–N5	1.37	1.39
N4–N5	1.34	1.32
C3–N4	1.34	1.37
C3–C8	1.47	1.43
C8–C18	1.40	1.42
C17–C18	1.39	1.37
C16–C17	1.40	1.43
C16–C19	1.48	1.44
C19–C20	1.41	1.43
C20–C21	1.39	1.37
C21–C22	1.40	1.42
C22–C25	1.43	1.41
C25–N26	1.16	1.16

Table 8 Experimental data and TD-DFT calculations (CAM-B3LYP 6-311G(d,p)) of the absorption and emission maxima for pyrazole **5d** in dichloromethane

	Experimental [nm]	Computed [nm]	Transition dipole moment
$\lambda_{max,abs}$ (**5d**)	281	256 (HOMO → LUMO (50%))	10.6
$\lambda_{max,em}$ (**5d**)	352	340	20.6

central pyrazole core. This is different with respect to simple substituted and annellated pyrazoles where butterfly and kite conformations are considered to be the origin of large Stokes shifts.[19] The vibrationally relaxed ground state (S_0) geometry, optimized with Gaussian09 with a similar basis set employing dichloromethane as a solvent, differs at first glance from the geometry of the excited state only in the dihedral angle between the two rings of the biaryl substituent. As a consequence of excitation the biphenyl moiety planarizes with a torsional angle $\theta_{calc.,exc} = 13^\circ$ ($\theta_{calc.,ground} = 36^\circ$). A closer inspection of the optimized vibrationally relaxed S_1 state structure reveals far more distinct geometry changes. In the pyrazole core the nitrogen–nitrogen bond N4–N5 is contracted, whereas the nitrogen–carbon bonds C1–N5 and C3–N4 are elongated upon excitation (Fig. 9, Table 7).

In addition, the carbon–carbon bonds in the biaryl residue indicate rather bond length alternation between single and double bonds than typical aromatic bond lengths. This also plausibly rationalizes the biphenyl planarization upon excitation. Also the carbon–carbon bond C22–C25 ligating the nitrile group to the phenylene moiety is slightly contracted to 1.41 Å. While the pyrazole nitrogen atom N5 bears a partial charge of −0.30 in the ground state, it is slightly positively charged (0.08) in the excited state. However, nitrogen atom N4 is obviously not affected by this charge transfer. Yet, adjacent carbon atoms to the nitrogen atoms reveal an inverse behavior. In the nitrile group with nitrogen atom N26 receives a lower negative partial charge in the excited state whereas the partial charge of the nitrile carbon atom C25 alters from positive to negative. In conclusion the dipolar nature of the first excited state of **6d** is evident (Fig. 9).

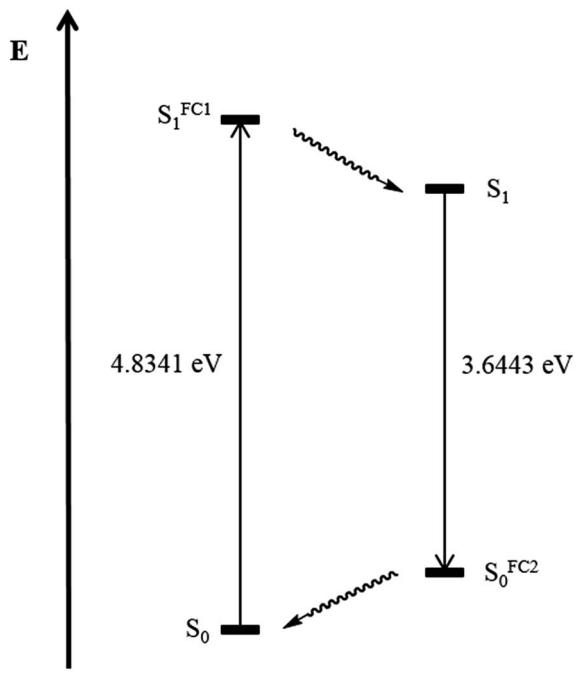

Fig. 10 Theoretical results for pyrazole **5d** depicted schematically for the excitation to the Franck–Condon state S_1^{FC1}, internal conversion to the relaxed S_1 state, emission to the Franck–Condon state S_0^{FC2} and relaxation to S_0 state after PCM correction (dichloromethane).

The calculation of the emission maximum of **6d** of $\lambda_{em,calc.} = 374$ nm, performed with Turbomole with TZVP on the geometry optimized structure of the excited state as confirmed by a numerical frequency analysis,[36] reproduces the experimental value of $\lambda_{em,exp} = 385$ nm in good agreement. The measured and the computed absorption maximum of pyrazole **5d** are representative for this class of pyrazoles. In this case the dominant contribution arises from the HOMO → LUMO transition (Table 8).

In addition the geometry of the vibrationally relaxed excited state (S_1)[31] of structure **5d** was optimized with Gaussian09 with a similar basis set employing dichloromethane as a solvent. The calculation of the emission maximum of pyrazole **5d** of $\lambda_{em,calc.} = 340$ nm, reproduces the experimental value of $\lambda_{em,exp} = 352$ nm in good agreement. Fig. 10 summarizes the results of the theoretical analysis. The transition dipole moment after excitation from the electronic ground state S_0 to the Franck–Condon state S_1^{FC1} ($\Delta\mu = 10.6$ SI) differs extremely from the transition dipole moment from the electronic relaxed excited state S_1 to the Franck–Condon state S_0^{FC2} ($\Delta\mu = 20.1$ SI).

Conclusions

A microwave-assisted consecutive four-component synthesis of biarylsubstituted pyrazoles based upon a sequentially Pd-catalyzed coupling–condensation–coupling (C^3) was successfully established. A particular feature of this one-pot sequence is the sequential use of the palladium catalyst without further catalyst addition for both the Sonogashira alkynylation and the Suzuki arylation. The absorption and emission properties can be tailored, fine-tuned and optimized towards high fluorescence quantum yields as a consequence of the diversity oriented nature of this process. Indeed, biaryl substituents improve the overall favorable photophysical properties of arylsubstituted pyrazoles giving rise to bright blue solution emissive molecular materials. Most favorably for achieving a redshifted emission with concomitant high fluorescence quantum yields the biaryl substituents should be placed in position 5 or 3 of the pyrazole core. The electronic structure of the first excited state can be

plausibly rationalized and also reproduced by ground and excited state computations on the DFT level of theory. Further studies directed to exploit this novel synthetic approach and the efficient option of optimizing the electronic properties in functional organic materials and also in matrices are currently underway.

Experimental

General considerations

All reactions were carried out in flame-dried glassware under nitrogen atmosphere. Reagents and catalyst were purchased reagent-grade and used without further purification. Besides triethylamine was dried with calcium hydride and stored over potassium hydroxide under nitrogen atmosphere. Solvents were dried by a solvent purification system. Dielectric heating was performed in a single mode microwave cavity producing continuous irradiation at 2450 MHz.

Further purification of the compounds was performed with flash column chromatography (silica gel 60, mesh 230–400). TLC: silica coated aluminium plates (60, F_{254}). ^{1}H, ^{13}C, DEPT and NOESY NMR spectra were recorded in $CDCl_3$, $CDCl_2$ or acetone-d_6 on 300 MHz (Bruker AVIII) or 600 MHz (Bruker Avance III-600) NMR spectrometers. The assignments of C_{quat}, CH, CH_2 and CH_3 nuclei were based on DEPT spectra. The elemental analyses were carried out in the microanalytical laboratory on a Perkin Elmer Series II Analyser 2400 of the Pharmazeutisches Institut of the Heinrich-Heine-Universität Düsseldorf. Mass spectra were recorded with a GC/MS-spectrometer Finnigan Trace DSQ with Finnigan Trace GC Ultra (Thermo Electron Corp.) or the ESI spectrometer Ion-Trap-API-mass spectrometer Finnigan LCQDeca (Thermo Quest). High resolution mass spectra were measured on a UHR-QTOF maxis 4G (Bruker Daltonics). Infrared spectra were recorded with a Shimadzu IR Affinity-1 with ATR technique. The intensities of signals are abbreviated as s (strong), m (medium) and w (weak). Absorption spectra were recorded in CH_2Cl_2 or cyclohexane UVASOL at 293 K on Perkin Elmer UV/VIS/NIR Lambda 19 Spectrometer. Emission spectra were recorded in CH_2Cl_2 or cyclohexane UVASOL at 293 K on a Perkin Elmer LS55 spectrometer. The melting points were determined with Reichert Thermovar with Kofler technique and they were not corrected.

Synthetic procedures

General procedure for the one-pot synthesis of 5-biarylsubstituted pyrazoles 5 (GP1). In a 10 mL microwave tube $PdCl_2(PPh_3)_2$ (14 mg, 0.02 mmol) and CuI (7.62 mg, 0.04 mmol) were dissolved in THF (4.0 mL) under nitrogen. To the yellow solution the acid chloride **1** (1.0 mmol) and the alkyne **2a** (1.05 mmol) were added (for experimental details see Table 9). Finally triethylamine (106 mg, 1.05 mmol) was added. The reaction mixture turned from yellow to light brown and stirring at room temperature was continued for 2 h. Then the hydrazine **3** (1.1 mmol) was added and the reaction mixture was stirred under continuous microwave irradiation at 150 °C for 20 min. After cooling to room temperature the boronic acid **4** (1.5 mmol), Cs_2CO_3 (978 mg, 3.00 mmol) dissolved in deionized water (1.0 mL) and PPh_3 (53 mg, 0.2 mmol) were added. The reaction mixture was stirred under microwave irradiation at 120 °C for 1 h. After cooling to room temperature the reaction mixture was extracted with dichloromethane (3 × 20 mL) and then washed with a saturated aqueous solution of ammonium chloride and brine. The combined organic layers were dried with anhydrous magnesium sulfate. The crude products were purified by flash chromatography (*n*-hexane/ethyl acetate 20 : 1 (v/v)) to give the desired pyrazoles **5**.

1-Methyl-5-(4′-methyl-[1,1′-biphenyl]-4-yl)-3-phenyl-1*H*-pyrazole (5a). According to GP1 217 mg (67%) of compound **5a** were obtained as a yellow solid; Mp 122 °C. ^{1}H NMR (300 MHz, $CDCl_3$) δ = 2.43 (s, 3H), 3.99 (s, 3H), 6.66 (s, 1H), 7.28–7.34 (m, 3H), 7.42 (t, J = 7.4 Hz, 2H), 7.50–7.59 (m, 4H), 7.70 (d, J = 8.5 Hz, 2H), 7.85 (d, J = 7.0 Hz, 2H). ^{13}C NMR (75 MHz, $CDCl_3$) δ = 21.3 (CH_3), 37.8 (CH_3), 103.4 (CH), 125.7 (CH), 127.1 (CH), 127.3 (CH), 127.8 (CH), 128.8 (CH), 129.2 (CH), 129.4 (C_{quat}), 129.8 (CH), 133.6 (C_{quat}), 137.5 (C_{quat}), 137.8 (C_{quat}), 141.5 (C_{quat}), 145.0 (C_{quat}), 150.7 (C_{quat}). IR (ATR): $\tilde{\nu}$ [cm^{-1}] 3024 (w), 2980 (w), 2918 (w), 1601 (w), 1485 (m), 1460 (m), 1438 (w), 1358 (w), 1290 (w), 1188 (w), 1115 (w), 1002 (m), 954 (m), 912 (w), 853 (m), 814 (s), 793 (s), 762 (s), 739 (m), 687 (s), 671 (m). GC-MS (*m*/*z* (%)): 326 (2), 325 (25), 324 ([M^+], 100), 321 (2), 320 (3), 294 (2), 239 (2), 215 (4), 194 (4), 193 (7), 192 (3), 171 (3), 162 (15), 161 (4), 154 (4), 153 (3), 130 (3), 118 (3), 117 (3), 104 (3), 89 (3), 77 (5). UV/Vis (CH_2Cl_2): λ_{max} [nm] (ε [L cm^{-1} mol^{-1}]) = 273.5 (40 100). Emission (CH_2Cl_2): λ_{max} [nm] (Φ_f) = 357.0 (0.77). Stokes shift [cm^{-1}] = 9400. Anal. calcd for $C_{23}H_{20}N_2$ (324.4): C 85.15, H 6.21, N 8.63; found C 85.23, H 6.17, N 8.75%.

Table 9 Experimental details for the one-pot synthesis of 5-biarylsubstituted pyrazoles **5**

Entry	Acid chloride **1** mg (mmol)	Alkyne **2a** mg (mmol)	Hydrazine **3** mg (mmol)	Boronic acid **4** mg (mmol)	5-Biarylsubstituted pyrazoles **5** mg (%)
1	142 (1.00) of **1a**	182 (1.05) of **2a**	51.9 (1.10) of **3a**	204 (1.50) of **4a**	217 (67) of **5a**
2	141 (1.00) of **1a**	182 (1.05) of **2a**	50.9 (1.10) of **3a**	183 (1.50) of **4b**	229 (76) of **5b**
3[a]	281 (2.00) of **1a**	362 (2.00) of **2a**	101.4 (2.20) of **3a**	464 (3.00) of **4c**	451 (66) of **5c**
4	160 (1.00) of **1b**	182 (1.05) of **2a**	51.4 (1.10) of **3a**	205 (1.50) of **4a**	100 (29) of **5d**
5	148 (1.00) of **1c**	181 (1.05) of **2a**	53.0 (1.10) of **3a**	205 (1.50) of **4a**	227 (69) of **5e**
6	150 (1.00) of **1c**	183 (1.05) of **2a**	52.4 (1.10) of **3a**	229 (1.50) of **4d**	147 (43) of **5f**
7	141 (1.00) of **1a**	181 (1.05) of **2a**	56.1 (1.10) of **3b**	205 (1.50) of **4a**	140 (45) of **5g**

[a] $PdCl_2(PPh_3)_2$ (28.0 mg, 0.04 mmol), CuI (15.4 mg, 0.08 mmol), Et_3N (207.4 mg, 2.05 mmol), Cs_2CO_3 (1.95 g, 4.50 mmol), PPh_3 (104.1 mg, 0.40 mmol).

5-([1,1′-Biphenyl]-4-yl)-1-methyl-3-phenyl-1*H*-pyrazole (5b). According to GP1 229 mg (76%) of compound **5b** were obtained as a yellow solid; Mp 112 °C. ^{1}H NMR (600 MHz, $CDCl_3$) δ = 3.99 (s, 3H), 6.67 (s, 1H), 7.33 (t, J = 7.4 Hz, 1H), 7.39–7.44 (m, 3H), 7.49 (t, J = 7.7 Hz, 2H), 7.56 (d, J = 8.3 Hz, 2H), 7.66 (d, J = 7.2 Hz, 2H), 7.72 (d, J = 8.3 Hz, 2H), 7.87 (d, J = 7.2 Hz, 2H). ^{13}C NMR (151 MHz, $CDCl_3$) δ = 37.9 (CH_3), 103.4 (CH), 125.7 (CH), 127.2 (CH), 127.5 (CH), 127.8 (CH), 127.9 (CH), 128.8 (CH), 129.1 (CH), 129.2 (CH), 129.6 (C_{quat}), 133.5 (C_{quat}), 140.4 (C_{quat}), 141.5 (C_{quat}), 144.9 (C_{quat}), 150.7 (C_{quat}). IR (ATR): $\tilde{\nu}$ [cm^{-1}] 3028 (w), 2936 (w), 1601 (w), 1483 (m), 1460 (m), 1439 (w), 1360 (w), 1279 (w), 1186 (w), 1113 (w), 1003 (m), 957 (w), 918 (w), 849 (m), 799 (m), 766 (s), 737 (m), 694 (s), 675 (m). EI-MS (m/z (%)): 311.1 (31), 310 ([M^+], 100), 273 (3), 232 (5), 179 (6), 155 (9), 135 (7), 116 (3), 77 (5). UV/Vis (CH_2Cl_2): λ_{max} [nm] (ε [L cm^{-1} mol^{-1}]) = 268.5 (36 700). Emission (CH_2Cl_2): λ_{max} [nm] (Φ_f) = 359.0 (0.77). Stokes shift [cm^{-1}] = 8600. Anal. calcd for $C_{22}H_{18}N_2$ (310.4): C 85.13, H 5.85, N 9.03; found C 84.92, H 5.88, N 8.77%.

5-(4′-Fluoro-2′-methyl-[1,1′-biphenyl]-4-yl)-1-methyl-3-phenyl-1*H*-pyrazole (5c). According to GP1 451 mg (66%) of compound **5c** were obtained as a light yellow solid; Mp 124 °C. ^{1}H NMR (300 MHz, $CDCl_3$) δ = 2.32 (s, 3H), 4.00 (s, 3H), 6.67 (s, 1H), 6.93–7.05 (m, 2H), 7.23 (dd, J = 8.4, 6.0 Hz, 1H), 7.33 (d, J = 7.4 Hz, 1H), 7.38–7.46 (m, 4H), 7.47–7.54 (m, 2H), 7.82–7.89 (m, 2H). ^{13}C NMR (75 MHz, $CDCl_3$) δ = 20.8 (CH_3, d, J = 1.4 Hz), 37.9 (CH_3), 103.5 (CH), 112.9 (CH, d, J = 21.1 Hz), 117.1 (CH, d, J = 21.0 Hz), 125.7 (CH), 127.79 (CH), 128.6 (CH), 128.8 (CH), 129.4 (C_{quat}), 129.8 (CH), 131.3 (C_{quat}, d, J = 8.3 Hz), 133.5 (C_{quat}), 137.2 (C_{quat}, d, J = 3.1 Hz), 137.9 (d, J = 7.8 Hz), 141.4 (C_{quat}), 144.9 (C_{quat}), 150.7 (C_{quat}), 162.3 (C_{quat}, d, J = 246.0 Hz). IR (ATR): $\tilde{\nu}$ [cm^{-1}] 3026 (w), 2940 (w), 1609 (w), 1481 (m), 1460 (m), 1439 (w), 1360 (w), 1269 (m), 1223 (m), 1192 (w), 1150 (m), 1119 (w), 1003 (m), 955 (m), 909 (w), 850 (m), 799 (m), 766 (s), 685 (s), 683 (m). GC-MS (m/z (%)): 343 ([M^+ + H], 25), 342 ([M^+], 100), 183 ([$C_{13}H_{10}F^+$], 13), 157 ([$C_{10}H_9N_2$], 7), 118 ([$C_8H_5F^+$], 22), 91 ([$C_7H_7^+$], 9), 77 ([$C_6H_5^+$], 19), 65 ([$C_5H_5^+$], 2), 51 ([$C_4H_3^+$], 4). UV/Vis (CH_2Cl_2): λ_{max} [nm] (ε [L cm^{-1} mol^{-1}]) = 263.0 (38 400). Emission (CH_2Cl_2): λ_{max} [nm] (Φ_f) = 344.5 (0.67). Stokes shift [cm^{-1}] = 9000. Anal. calcd for $C_{23}H_{19}N_2F$ (342.4): C 80.68, H 5.59, N 8.18; found C 80.58, H 5.52, N 7.9%.

3-(2-Fluorophenyl)-1-methyl-5-(4′-methyl-[1,1′-biphenyl]-4-yl)-1*H*-pyrazole (5d). According to GP1 100 mg (29%) of compound **5d** were obtained as a light yellow solid; Mp 132 °C. ^{1}H NMR (300 MHz, $CDCl_3$) δ = 2.42 (s, 3H), 4.00 (s, 3H), 6.81 (d, J_{H-F} = 3.9 Hz, 1H), 7.08–7.24 (m, 2H), 7.29 (d, J = 8.3 Hz, 3H), 7.55 (d, J = 6.7 Hz, 4H), 7.69 (d, J = 8.5 Hz, 2H), 8.04 (td, J = 7.7 Hz, 1.9 Hz, 1H). ^{13}C NMR (75 MHz, $CDCl_3$) δ = 21.3 (CH_3), 37.9 (CH_3), 106.9 (CH, d, J = 9.6 Hz), 116.2 (CH, d, J = 22.3 Hz), 121.3 (C_{quat}), 121.5 (C_{quat}), 124.4 (CH, d, J = 3.4 Hz), 127.1 (CH), 127.3 (CH), 128.4 (CH, d, J = 3.8 Hz), 129.0 (CH, d, J = 8.3 Hz), 129.3 (CH), 129.8 (CH), 137.5 (C_{quat}), 137.7 (C_{quat}), 141.5 (C_{quat}), 144.6 (C_{quat}), 145.2 (C_{quat}), 160.2 (C_{quat}, d, J = 249.2 Hz). IR (ATR): $\tilde{\nu}$ [cm^{-1}] 3022 (w), 2345 (w), 1481 (m), 1468 (m), 1433 (w), 1354 (w), 1258 (w), 1206 (w), 1190 (w), 1043 (w), 961 (w), 854 (m), 808 (s), 756 (s), 737 (m), 692 (m). GC-MS (m/z (%)): 343 ([M^+ + H], 25), 342 ([M^+], 100), 299 ([$C_{23}H_{17}N_2F^+$], 4), 206 (2), 193 (4), 181 (3), 178 (3), 171 (15), 165 (4), 152 (3), 148 (2), 136 (2), 122 (4), 102 (3). UV/Vis (CH_2Cl_2): λ_{max} [nm] (ε [L cm^{-1} mol^{-1}]) = 281.0 (34 200). Emission (CH_2Cl_2): λ_{max} [nm] (Φ_f) = 351.5 (0.97). Stokes shift [cm^{-1}] = 7100. Anal. calcd for $C_{23}H_{19}N_2F$ (342.4): C 80.68, H 5.59, N 8.18; found C 79.08, H 5.43, N 8.01%.

1-Methyl-5-(4′-methyl-[1,1′-biphenyl]-4-yl)-3-(thiophen-2-yl)-1*H*-pyrazole (5e). According to GP1 227 mg (69%) of compound **5e** were obtained as a colorless light yellow solid; Mp 130 °C. ^{1}H NMR (600 MHz, $CDCl_3$) δ = 2.43 (s, 3H), 3.95 (s, 3H), 6.57 (s, 1H), 7.05–7.10 (m, 1H), 7.26 (d, J = 4.3 Hz, 1H), 7.30 (d, J = 7.8 Hz, 2H), 7.36 (d, J = 3.5 Hz, 1H), 7.52 (d, J = 8.3 Hz, 2H), 7.55 (d, J = 8.0 Hz, 2H), 7.69 (d, J = 8.2 Hz, 2H). ^{13}C NMR (151 MHz, $CDCl_3$) δ = 21.3 (CH_3), 37.8 (CH_3), 103.3 (CH), 123.6 (CH), 124.4 (CH), 127.0 (CH), 127.6 (CH), 127.3 (CH), 129.0 (CH), 129.2 (CH), 129.8 (C_{quat}), 136.8 (C_{quat}), 137.4 (C_{quat}), 137.8 (C_{quat}), 141.6 (C_{quat}), 144.9 (C_{quat}), 146.0 (C_{quat}). IR (ATR): $\tilde{\nu}$ [cm^{-1}] 3019 (w), 2930 (w), 1489 (m), 1477 (m), 1439 (m), 1396 (m), 1375 (m), 1285 (m), 1221 (m, C–S), 1180 (w), 1105 (w), 1005 (m), 843 (m), 795 (s), 741 (m), 694 (s), 681 (m). GC-MS (m/z (%)): 330 ([M^+], 100), 287 (7), 239 ([$C_{14}H_{11}N_2S^+$], 2), 165 ([$C_{13}H_9^+$], 18), 91 ([$C_7H_7^+$], 8), 77 ([$C_6H_5^+$], 2), 65 ([$C_5H_5^+$], 4), 51 ([$C_4H_3^+$], 3). UV/Vis (CH_2Cl_2): λ_{max} [nm] (ε [L cm^{-1} mol^{-1}]) = 285.0 (44 000). Emission (CH_2Cl_2): λ_{max} [nm] (Φ_f) = 382.0 (0.35). Stokes shift [cm^{-1}] = 8900. Anal. calcd for $C_{21}H_{18}N_2S$ (330.5): C 76.33, H 5.49, N 8.48; found C 76.11, H 5.35, N 8.47%.

5-(4′-Methoxy-[1,1′-biphenyl]-4-yl)-1-methyl-3-(thiophen-2-yl)-1*H*-pyrazole (5f). According to GP1 147 mg (43%) of compound **5f** were obtained as a light yellow solid; Mp 117 °C. ^{1}H NMR (300 MHz, $CDCl_3$) δ = 3.87 (s, 3H), 3.94 (s, 3H), 6.55 (s, 1H), 7.01 (d, J = 8.8 Hz, 2H), 7.07 (dd, J = 5.1 Hz, 3.6, 1H), 7.25 (dd, J = 4.9 Hz, 1.2, 1H), 7.35 (dd, J = 3.5, 1.1 Hz, 1H), 7.50 (d, J = 8.4 Hz, 2H), 7.58 (d, J = 8.8 Hz, 2H), 7.66 (d, J = 8.4 Hz, 2H). ^{13}C NMR (75 MHz, $CDCl_3$) δ = 37.8 (CH_3), 55.5 (CH_3), 103.3 (CH), 114.5 (CH), 123.6 (CH), 124.4 (CH), 127.0 (CH), 127.6 (CH), 128.3 (CH), 128.7 (C_{quat}), 129.2 (CH), 132.8 (C_{quat}), 136.8 (C_{quat}), 141.2 (C_{quat}), 145.0 (C_{quat}), 146.0 (C_{quat}), 159.7 (C_{quat}). IR (ATR): $\tilde{\nu}$ [cm^{-1}] 3030 (w), 2938 (w), 2839 (w), 1603 (m), 1516 (m), 1487 (m), 1443 (m), 1369 (w), 1285 (m), 1261 (m), 1248 (m), 1178 (m), 1117 (w), 1026 (m), 1001 (m), 920 (m), 849 (m), 810 (s), 779 (s), 752 (w), 700 (s), 642 (m). GC-MS (m/z (%)): 348 (8). 347 (24), 346 (100), 332 (5), 331 (23), 304 (3), 303 (15), 258 (2), 174 (2), 173 (16), 152 (19), 139 (4), 130 (3), 117 (3), 110 (2). UV/Vis (CH_2Cl_2): λ_{max} [nm] (ε [L cm^{-1} mol^{-1}]) = 289.0 (43 300). Emission (CH_2Cl_2): λ_{max} [nm] (Φ_f) = 363.0 (0.80). Stokes shift [cm^{-1}] = 7100. Anal. calcd for $C_{21}H_{18}N_2OS$ (346.5): C 72.80, H 5.24, N 8.09; found C 72.62, H 5.01, N 7.86%.

5-(4′-Methyl-[1,1′-biphenyl]-4-yl)-3-phenyl-1*H*-pyrazole (5g). According to GP1 140 mg (45%) of compound **5g** were obtained as a colorless solid; Mp 189 °C. ^{1}H NMR (300 MHz, acetone-d_6) δ = 2.37 (s, 3H), 7.17 (s, 1H), 7.29 (d, J = 7.9 Hz, 2H), 7.36 (d, J = 7.3 Hz, 1H), 7.46 (t, J = 7.5 Hz, 2H), 7.61 (d, J = 8.2 Hz, 2H), 7.73 (d, J = 8.4 Hz, 2H), 7.90 (d, J = 7.2 Hz, 2H), 7.96 (d, J = 8.4 Hz, 2H), 12.59 (s, 1H). ^{13}C NMR (75 MHz, acetone-d_6) δ = 21.1 (CH_3), 100.4 (CH), 126.2 (CH), 126.6 (CH), 127.4 (CH), 127.8 (CH), 128.7 (CH), 129.7 (CH), 130.4 (CH), 138.0 (3 C_{quat}), 138.4 (2 C_{quat}), 141.1 (2 C_{quat}). IR (ATR): $\tilde{\nu}$ [cm^{-1}] 3030 (w), 2940 (w), 2859 (w), 1605 (w), 1489 (m), 1458 (m), 1377 (w), 1290 (w), 1180 (m), 1115 (w), 1005 (w), 968 (m), 849 (m), 814 (s), 795 (s), 762 (s), 741 (w),

689 (s). EI-MS (*m*/*z* (%)): 311 ([M^+], 21), 310 (100), 298 (6), 281 (6), 265 (6), 189 (4), 165 (7), 155 (9), 154 (5), 140 (3), 104 (2), 89 (2), 77 (2). UV/Vis (CH_2Cl_2): λ_{max} [nm] (ε [L cm^{-1} mol^{-1}]) = 285.0 (42 000). Emission (CH_2Cl_2): λ_{max} [nm] (Φ_f) = 343.5 (0.86). Stokes shift [cm^{-1}] = 6000. HRMS calcd for $C_{22}H_{18}N_2$ + H^+: 311.1543; found 311.1546.

General procedure for the one-pot synthesis of 3-biarylsubstituted pyrazoles 6 (GP2). In a 10 mL microwave tube $PdCl_2(PPh_3)_2$ (14.0 mg, 0.02 mmol) and CuI (7.62 mg, 0.04 mmol) were dissolved in 1,4-dioxane (4 mL) under nitrogen. To the yellow solution acid chloride (**1d**) (226 mg, 1.00 mmol) and the alkyne **2** (1.0 mmol) were added (for experimental details see Table 10). Finally triethylamine (106 mg, 1.05 mmol) was added. The reaction mixture turned from yellow to light brown and was stirred at room temperature for 2 h. Then methylhydrazine (**3a**) (51.3 mg, 1.10 mmol) was added and the reaction mixture was stirred under continuous microwave irradiation at 150 °C for 20 min. After cooling to room temperature the boronic acid **4** (1.5 mmol), Cs_2CO_3 (978 mg, 3.00 mmol) dissolved in deionized water (1.0 mL) and PPh_3 (53 mg, 0.2 mmol) were added. The reaction mixture was stirred under continuous microwave irradiation at 120 °C for 1 h. After cooling to room temperature the reaction mixture was extracted with dichloromethane (3 × 20 mL) and then washed with a saturated aqueous solution of ammonium chloride and brine. The combined organic layers were dried with anhydrous magnesium sulfate. The crude products were purified by flash chromatography (*n*-hexane/ethyl acetate 10 : 1 (v/v)) to give the desired pyrazoles **6**.

3-([1,1′-Biphenyl]-4-yl)-1-methyl-5-phenyl-1*H*-pyrazole (6a). According to GP2 207 mg (66%) of compound **6a** were obtained as a light yellow solid; Mp 101 °C. ^{1}H NMR (300 MHz, $CDCl_3$) δ = 3.96 (s, 3H), 6.66 (s, 1H), 7.29–7.54 (m, 8H), 7.66 (d, J = 8.5 Hz, 4H), 7.92 (d, J = 8.5 Hz, 2H). ^{13}C NMR (75 MHz, $CDCl_3$) δ = 37.8 (CH_3), 103.4 (CH), 126.0 (CH), 127.1 (CH), 127.4 (CH), 127.5 (CH), 128.7 (CH), 128.87 (CH), 128.90 (4 CH), 130.8 (C_{quat}), 132.6 (C_{quat}), 140.4 (C_{quat}), 141.0 (C_{quat}), 145.3 (C_{quat}), 150.3 (C_{quat}). IR (ATR): $\tilde{\nu}$ [cm^{-1}] 3030 (w), 2926 (w), 1598 (w), 1578 (w), 1481 (m), 1460 (m), 1352 (w), 1279 (w), 1188 (w), 1119 (w), 1007 (m), 957 (m), 918 (w), 847 (m), 791 (m), 768 (s), 760 (s), 694 (s). GC-MS (*m*/*z* (%)): 311 (25), 310 ([M^+], 100), 265 (3), 179 (3), 178 (2), 155 (13), 152 (5), 130 (3), 118 (10), 103 (5), 91 (4), 77 (9). UV/Vis (CH_2Cl_2): λ_{max} [nm] (ε [L cm^{-1} mol^{-1}]) = 283.5 (35 600). Emission (CH_2Cl_2): λ_{max} [nm] (Φ_f) = 344.5 (0.49). Stokes shift [cm^{-1}] = 6300. Anal. calcd for $C_{22}H_{18}N_2$ (310.4): C 85.13, H 5.85, N 9.03; found C 84.92, H 5.88, N 8.77%.

3-(4′-Fluoro-2′-methyl-[1,1′-biphenyl]-4-yl)-1-methyl-5-(*p*-tolyl)-1*H*-pyrazole (6b). According to GP2 274.3 mg (51%) of compound **6b** were obtained as a light orange solid; Mp 157 °C. ^{1}H NMR (300 MHz, $CDCl_3$) δ = 2.29 (s, 3H), 2.44 (s, 3H), 3.95 (s, 3H), 6.62 (s, 1H), 6.94–7.00 (m, 2H), 7.18–7.25 (m, 1H), 7.28–7.41 (m, 5H), 7.52 (d, J = 8.3 Hz, 1H), 7.74 (d, J = 8.1 Hz, 1H), 7.87 (d, J = 8.4 Hz, 1H). ^{13}C NMR (75 MHz, $CDCl_3$) δ = 20.8 (CH_3), 21.4 (CH_3), 37.7 (CH_3), 103.2 (CH), 112.6 (CH, d, J = 20.9 Hz), 116.9 (CH, d, J = 21.0 Hz), 125.5 (CH), 128.8 (CH), 129.6 (CH), 129.7 (CH), 131.3 (CH, d, J = 8.2 Hz), 132.3 (C_{quat}), 137.5 (C_{quat}), 137.9 (C_{quat}, d, J = 11.3 Hz), 138.7 (C_{quat}), 140.3 (C_{quat}), 141.3 (C_{quat}), 145.3 (C_{quat}), 150.3 (C_{quat}), 162.1 (C_{quat}, d, J = 122.6 Hz). IR (ATR): $\tilde{\nu}$ [cm^{-1}] 3049 (w), 2951 (w), 1609 (w), 1585 (w), 1481 (m), 1437 (m), 1350 (w), 1265 (w), 1223 (m), 1007 (w), 943 (w), 854 (m), 822 (s), 787 (s), 745 (m), 691 (m). GC-MS (*m*/*z* (%)): 357 (26), 356 (100), 226 (2), 207 (2), 183 (6), 178 (11), 177 (5), 170 (5), 169 (2), 146 (2), 132 (4), 118 (3), 115 (3), 91 (5), 77 (2). UV/Vis (CH_2Cl_2): λ_{max} [nm] (ε [L cm^{-1} mol^{-1}]) = 267.5 (35 800). Emission (CH_2Cl_2): λ_{max} [nm] (Φ_f) = 338.5 (0.83). Stokes shift [cm^{-1}] = 7800. HRMS calcd for $C_{24}H_{21}FN_2$ + H^+: 357.1762; found 357.1763.

3-([1,1′-Biphenyl]-4-yl)-5-butyl-1-methyl-1*H*-pyrazole (6c). According to GP2 356.0 mg (61%) of compound **6c** were obtained as a light yellow solid; Mp 76 °C. ^{1}H NMR (300 MHz, $CDCl_3$) δ = 0.99 (t, J = 7.3 Hz, 3H), 1.40–1.52 (m, 2H), 1.64–1.74 (m, 2H), 2.36–2.76 (m, 2H), 3.85 (s, 3H), 6.37 (s, 1H), 7.35 (d, J = 7.4 Hz, 1H), 7.38–7.54 (m, 2H), 7.55–7.70 (m, 4H), 7.85 (d, J = 8.5 Hz, 1H). ^{13}C NMR (75 MHz, $CDCl_3$) δ = 14.0 (CH_3), 22.5 (CH_2), 25.6 (CH_2), 30.7 (CH_2), 36.3 (CH_3), 101.6 (CH), 125.9 (CH), 127.1 (CH), 127.3 (CH), 127.4 (CH), 128.9 (CH), 132.8 (C_{quat}), 140.2 (C_{quat}), 141.0 (C_{quat}), 144.8 (C_{quat}), 149.7 (C_{quat}). IR (ATR): $\tilde{\nu}$ [cm^{-1}] 3053 (w), 2953 (w), 2928 (w), 2859 (w), 1597 (w), 1491 (m), 1466 (m), 1439 (m), 1368 (w), 1292 (w), 1119 (w), 1007 (m), 959 (m), 847 (m), 806 (m), 785 (m), 764 (s), 729 (s), 696 (s). GC-MS (*m*/*z* (%)): 291 (14), 290 (61), 249 (18), 248 (100), 247 (70), 232 (2), 206 (3), 203 (8), 202 (12), 179 (4), 178 (5), 165 (3), 153 (3), 152 (7), 125 (3), 124 (26), 115 (2), 77 (2), 69 (4), 54 (2). UV/Vis (CH_2Cl_2): λ_{max} [nm] (ε [L cm^{-1} mol^{-1}]) = 286.0 (33 000). Emission (CH_2Cl_2): λ_{max} [nm] (Φ_f) = 347.0 (0.27). Stokes shift [cm^{-1}] = 6200. Anal. calcd for $C_{20}H_{22}N_2$ (290.4): C 82.72, H 7.64, N 9.65; found C 82.50, H 7.51, N 9.73%.

4′-(1-Methyl-5-phenyl-1*H*-pyrazol-3-yl)-[1,1′-biphenyl]-4-carbonitrile (6d). According to GP2 395 mg (59%) of compound **6d** were obtained as a colorless gleamy solid; Mp 214 °C. ^{1}H NMR (300 MHz, CD_2Cl_2) δ = 3.94 (s, 3H), 6.69 (s, 1H), 7.42–7.56 (m, 5H), 7.68 (d, J = 8.6 Hz, 2H), 7.75 (br, 5H), 7.95 (d, J = 8.6 Hz,

Table 10 Experimental details for the one-pot synthesis of 3-biarylsubstituted pyrazoles **6**

Entry	Acid chloride **1d** mg (mmol)	Alkyne **2** mg (mmol)	Methylhydrazine **3a** mg (mmol)	Boronic acid **4** mg (mmol)	3-Biarylsubstituted pyrazoles **6** mg (%)
1	226 (1.00) of **1d**	106.4 (1.00) of **2b**	51.3 (1.10)	183 (1.50) of **4b**	207 (66) of **6a**
2[a]	330 (1.50) of **1d**	179 (1.50) of **2c**	77.1 (1.70)	325 (2.10) of **4c**	274 (51) of **6b**
3[b]	444 (2.00) of **1d**	170 (2.00) of **2d**	104 (2.20)	367 (3.00) of **4b**	356 (61) of **6c**
4[b]	439 (2.00) of **1d**	205 (2.00) of **2b**	101 (2.20)	407 (2.80) of **4e**	395 (59) of **6d**

[a] $PdCl_2(PPh_3)_2$ (21.0 mg, 0.03 mmol), CuI (11.4 mg, 0.06 mmol), Et_3N (159 mg, 1.57 mmol), Cs_2CO_3 (1.47 g, 4.50 mmol), PPh_3 (79.1 mg, 0.30 mmol). [b] $PdCl_2(PPh_3)_2$ (28.0 mg, 0.04 mmol), CuI (15.2 mg, 0.08 mmol), Et_3N (212 mg, 2.10 mmol), Cs_2CO_3 (1.96 mg, 6.0 mmol), PPh_3 (105 mg, 0.40 mmol).

2H). ^{13}C NMR (75 MHz, CD_2Cl_2) δ = 38.3 (CH_3), 103.7 (CH), 111.35 (C_{quat}), 119.5 (C_{quat}), 126.5 (CH), 127.94 (CH), 127.98 (CH), 129.1 (CH), 129.2 (CH), 129.3 (CH), 131.1 (C_{quat}), 133.2 (CH), 134.6 (C_{quat}), 138.5 (C_{quat}), 145.65 (C_{quat}), 145.74 (C_{quat}), 149.7 (C_{quat}). IR (ATR): $\tilde{\nu}$ [cm^{-1}] 3038 (w), 2999 (w), 2949 (w), 2222 (m), 1603 (m), 1483 (m), 1472 (m), 1458 (m), 1437 (m), 1354 (w), 1283 (w), 1186 (m), 1119 (w), 1003 (w), 959 (m), 910 (w), 826 (s), 791 (s), 762 (s), 746 (m), 689 (m), 673 (m). EI/MS (*m*/*z* (%)): 337 (3), 336 (25), 335 (100), 334 (7), 292 (3), 290 (2), 204 (2), 167 (7), 151 (2), 118 (3), 103 (3), 77 (2), 44 (2), 43 (3). UV/Vis (CH_2Cl_2): λ_{max} [nm] (ε [L cm^{-1} mol^{-1}]) = 306.5 (36 600). Emission (CH_2Cl_2): λ_{max} [nm] (Φ_f) = 384.0 (0.10). Stokes shift [cm^{-1}] = 6600. Anal. calcd for $C_{23}H_{17}N_3$ (335.4): C 82.36, H 5.11, N 12.53; found C 82.18, H 4.81, N 12.40%.

One-pot synthesis of 3,5-di([1,1′-biphenyl]-4-yl)-1-methyl-1*H*-pyrazole (7). In a 10 mL microwave tube $PdCl_2(PPh_3)_2$ (14.5 mg, 0.02 mmol) and CuI (8.53 mg, 0.04 mmol) were dissolved in THF (4.00 mL) under nitrogen. To the yellow solution acid chloride (**1d**) (219 mg, 1.00 mmol) and alkyne (**2a**) (180 mg, 1.00 mmol) were added. Finally triethylamine (109 mg, 1.07 mmol) was added. The reaction mixture turned from yellow to light brown and was stirred at room temperature for 2 h. Then methylhydrazine (**3a**) (53.5 mg, 1.15 mmol) were added and the reaction mixture was stirred under continuous microwave irradiation at 150 °C for 20 min. After cooling to room temperature boronic acid **4b** (366 mg, 3.00 mmol), Cs_2CO_3 (2.00 g, 6.14 mmol) dissolved in deionized water (1.0 mL) and PPh_3 (53.0 mg, 0.20 mmol) were added. The reaction mixture was stirred under continuous microwave irradiation at 120 °C for 1 h. After cooling to room temperature the reaction mixture was extracted with dichloromethane (3 × 20 mL) and then washed with a saturated aqueous solution of ammonium chloride and brine. The combined organic layers were dried with anhydrous magnesium sulfate. The crude product was purified by flash chromatography (*n*-hexane/ethyl acetate 20 : 1, v/v) to give 142 mg (37%) of pyrazole **7** as beige colored plates; Mp 200 °C. ^{1}H NMR (300 MHz, $CDCl_3$) δ = 4.01 (s, 3H), 6.70 (s, 1H), 7.33–7.53 (m, 6H), 7.57 (d, J = 8.4 Hz, 2H), 7.61–7.70 (m, 6H), 7.72 (d, J = 8.4 Hz, 2H), 7.93 (d, J = 8.4 Hz, 2H). ^{13}C NMR (75 MHz, $CDCl_3$) δ = 37.9 (CH_3), 103.5 (CH), 126.1 (CH), 127.1 (CH), 127.3 (CH), 127.4 (CH), 127.5 (CH), 127.6 (CH), 127.88 (CH), 128.91 (CH), 129.1 (CH), 129.3 (CH), 129.6 (C_{quat}), 132.6 (C_{quat}), 140.4 (C_{quat}), 140.5 (C_{quat}), 141.0 (C_{quat}), 141.6 (C_{quat}), 145.0 (C_{quat}), 150.4 (C_{quat}). IR (ATR): $\tilde{\nu}$ [cm^{-1}] 3028 (w), 2938 (w), 1477 (m), 1437 (m), 1277 (w), 1184 (w), 1119 (w), 1001 (m), 959 (m), 918 (w), 847 (s), 826 (m), 785 (m), 762 (s), 729 (m), 692 (s), 671 (m). GC-MS (*m*/*z* (%)): 388 (5), 387 (31), 386 (100), 343 (5), 281 (3), 207 (9), 206 (2), 194 (6), 193 (22), 180 (4), 179 (10), 165 (5), 153 (3), 152 (7), 133 (2), 77 (3), 73 (4). UV/Vis (CH_2Cl_2): λ_{max} [nm] (ε [L cm^{-1} mol^{-1}]) = 288.5 (62 500). Emission (CH_2Cl_2): λ_{max} [nm] (Φ_f) = 367.0 (0.07). Stokes shift [cm^{-1}] = 7400. HRMS calcd for $C_{28}H_{22}N_2$+H^+: 387.1856; found 387.1856.

General procedure for the one-pot synthesis of 1-biarylsubstituted pyrazoles 8 (GP3). In a 10 mL microwave tube $PdCl_2(PPh_3)_2$ (28.4 mg, 0.04 mmol) and CuI (15.4 mg, 0.08 mmol) were dissolved in dichloromethane (4 mL) under nitrogen. To the yellow solution acid chloride **1** (2.00 mmol) and alkyne **2** (2.00 mmol) were added (for experimental details see Table 11). Finally triethylamine (207 mg, 4.10 mmol) was added. The reaction mixture turned from yellow to light brown and was stirred at room temperature for 16 h. Then the hydrochloride of hydrazine (**3c**) (492 mg, 2.20 mmol) was added and the reaction mixture was stirred under continuous microwave irradiation at 100 °C for 40 min. After cooling to room temperature boronic acid **4** (3.00 mmol), Cs_2CO_3 (2.00 g, 6.00 mmol) dissolved in deionized water (1.0 mL) and PPh_3 (104 mg, 0.40 mmol) were added. The reaction mixture was stirred under continuous microwave irradiation at 100 °C for 90 min. After cooling to room temperature the reaction mixture was extracted with dichloromethane (3 × 20 mL) and then washed with a saturated aqueous solution of ammonium chloride and brine. The combined organic layers were dried with anhydrous magnesium sulfate. The crude products were purified by flash chromatography (*n*-hexane/ethylacetate 200 : 1 (v/v)) to give the desired pyrazoles **8**.

1-([1,1′-Biphenyl]-4-yl)-3,5-diphenyl-1*H*-pyrazole (8a). According to GP3 212 mg (57%) of compound **8a** were obtained as a light orange solid; Mp 160 °C. ^{1}H NMR (300 MHz, $CDCl_3$) δ = 6.86 (s, 1H), 7.36 (br, 7H), 7.45–7.47 (m, 6H), 7.58–7.60 (m, 4H), 7.96 (d, J = 8.1 Hz, 2H). ^{13}C NMR (75 MHz, $CDCl_3$) δ = 105.5 (CH), 125.5 (CH), 126.0 (CH), 127.2 (CH), 127.66 (CH), 127.70 (CH), 128.2 (CH), 128.5 (CH), 128.7 (CH), 128.8 (CH), 128.9 (CH),

Table 11 Experimental details for the one-pot synthesis of 1-biarylsubstituted pyrazoles **8**

Entry	Acid chloride **1** mg (mmol)	Alkyne **2** mg (mmol)	Hydrazine **3c** mg (mmol)	Boronic acid **4** mg (mmol)	1-Biarylsubstituted pyrazoles **8** mg (%)
1[a]	143 (1.00) of **1a**	109 (1.10) of **2b**	246 (1.10) of **3c**	183 (1.50) of **4b**	212 (57) of **8a**
2	281 (2.00) of **1a**	204 (2.00) of **2b**	492 (2.20) of **3c**	411 (3.00) of **4a**	456 (59) of **8b**
3	285 (2.00) of **1a**	208 (2.00) of **2b**	492 (2.20) of **3c**	439 (3.00) of **4e**	494 (62) of **8c**
4	283 (2.00) of **1a**	209 (2.00) of **2b**	493 (2.20) of **3c**	385 (3.00) of **4f**	431 (55) of **8d**
5[b]	361 (2.10) of **1e**	211 (2.10) of **2b**	493 (2.20) of **3c**	417 (3.10) of **4a**	365 (44) of **8e**
6	345 (2.00) of **1f**	212 (2.10) of **2b**	493 (2.20) of **3c**	411 (3.00) of **4a**	159 (19) of **8f**
7	306 (2.00) of **1c**	209 (2.10) of **2b**	493 (2.20) of **3c**	409 (3.00) of **4a**	430 (55) of **8g**
8	286 (2.00) of **1a**	164 (2.00) of **2d**	493 (2.20) of **3c**	409 (3.00) of **4a**	440 (60) of **8h**

[a] $PdCl_2(PPh_3)_2$ (14.0 mg, 0.02 mmol), CuI (7.62 mg, 0.04 mmol), Et_3N (106 mg, 1.05 mmol), Cs_2CO_3 (978 mg, 3.00 mmol), PPh_3 (52.3 mg, 0.2 mmol). [b] $PdCl_2(PPh_3)_2$ (29.0 mg, 0.04 mmol), CuI (16.7 mg, 0.09 mmol), Et_3N (223 mg, 2.20 mmol), Cs_2CO_3 (2.05 g, 6.30 mmol), PPh_3 (110 mg, 0.42 mmol).

129.0 (CH), 130.8 (C_{quat}), 133.2 (C_{quat}), 139.4 (C_{quat}), 140.2 (C_{quat}), 140.3 (C_{quat}), 144.5 (C_{quat}), 152.2 (C_{quat}). IR (ATR): $\tilde{\nu}$ [cm^{-1}] 3061 (w), 3032 (w), 1960 (w), 1896 (w), 1819 (w), 1605 (m), 1524 (m), 1487 (m), 1462 (m), 1435 (w), 1361 (m), 1217 (w), 1186 (w), 972 (m), 955 (m), 916 (m), 839 (m), 760 (s), 729 (m), 690 (s), 656 (m). GC-MS (*m*/*z* (%)): 373 (29), 372 (100), 344 (3), 295 (7), 268 (16), 267 (10), 254 (3), 241 (8), 166 (8), 152 (40), 151 (12), 139 (8), 115 (7), 103 (6), 102 (7), 90 (4), 89 (12), 77 (49), 51 (16). UV/Vis (CH_2Cl_2): λ_{max} [nm] (ε [L cm^{-1} mol^{-1}]) = 257.0 (36 300), 293.0 sh (25 000). Emission (CH_2Cl_2): λ_{max} [nm] (Φ_f) = 385.0 (0.41). Stokes shift [cm^{-1}] = 8200. Anal. calcd for $C_{27}H_{20}N_2$ (372.5): C 87.07, H 5.41, N 7.52; found: C 86.85, H 5.17, N 7.54%.

1-(4′-Methyl-[1,1′-biphenyl]-4-yl)-3,5-diphenyl-1*H*-pyrazole (8b). According to GP3 456 mg (59%) of compound **8b** were obtained as a light yellow solid; Mp 110 °C. ^{1}H NMR (300 MHz, $CDCl_3$) δ = 2.41 (s, 3H). 6.86 (s, 1H), 7.26 (d, J = 7.9 Hz, 2H), 7.36 (br, 6H), 7.40–7.46 (m, 4H), 7.50 (d, J = 8.2 Hz, 2H), 7.57 (d, J = 8.6 Hz, 2H), 7.96 (d, J = 7.0 Hz, 2H). ^{13}C NMR (75 MHz, $CDCl_3$) δ = 21.3 (CH_3), 105.4 (CH), 125.5 (CH), 126.0 (CH), 127.0 (CH), 127.4 (CH), 128.1 (CH), 128.5 (CH), 128.7 (CH), 128.8 (CH), 128.9 (CH), 129.7 (CH), 130.8 (C_{quat}), 133.2 (C_{quat}), 137.4 (C_{quat}), 137.5 (C_{quat}), 139.2 (C_{quat}), 140.2 (C_{quat}), 144.5 (C_{quat}), 152.1 (C_{quat}). IR (ATR): $\tilde{\nu}$ [cm^{-1}] 3026 (w), 2961 (w), 2916 (w), 1485 (m), 1460 (m), 1362 (m), 1267 (w), 1171 (w), 1005 (w), 972 (m), 955 (w), 916 (w), 849 (w), 808 (s), 760 (s), 733 (w), 692 (s). GC-MS (*m*/*z* (%)): 386 ([M^+], 100), 282 (15), 165 ([$C_{13}H_9^+$], 25), 91 ([$C_7H_7^+$], 5), 77 ([$C_6H_5^+$], 24), 65 ([$C_5H_5^+$], 6), 51 ([$C_4H_3^+$], 8). UV/Vis (CH_2Cl_2): λ_{max} [nm] (ε [L cm^{-1} mol^{-1}]) = 257.0 (32 000), 296.0 sh (23 000). Emission (CH_2Cl_2): λ_{max} [nm] (Φ_f) = 388.0 (0.33). Stokes shift [cm^{-1}] = 8000. Anal. calcd for $C_{28}H_{22}N_2$ (386.5): C 87.01, H 5.74, N 7.25; found: C 86.83, H 5.91, N 7.51%.

4′-(3,5-Diphenyl-1*H*-pyrazol-1-yl)-[1,1′-biphenyl]-4-carbonitrile (8c). According to GP3494 mg (62%) of compound **8c** were obtained as a colorless light yellow solid; Mp 156 °C. ^{1}H NMR (300 MHz, $CDCl_3$) δ = 6.86 (s, 1H), 7.30–7.42 (m, 6H), 7.44 (d, J = 7.5 Hz, 2H), 7.49 (d, J = 8.8 Hz, 2H), 7.57 (d, J = 8.8 Hz, 2H), 7.65–7.77 (m, 4H), 7.94 (d, J = 7.0 Hz, 2H). ^{13}C NMR (75 MHz, $CDCl_3$) δ = 105.9 (CH), 111.3 (C_{quat}), 119.0 (C_{quat}), 125.6 (CH), 126.0 (CH), 127.7 (CH), 127.8 (CH), 128.3 (CH), 128.7 (CH), 128.77 (CH), 128.83 (CH), 128.9 (CH), 130.6 (CH), 132.8 (C_{quat}), 133.0 (C_{quat}), 137.9 (C_{quat}), 140.6 (C_{quat}), 144.57 (C_{quat}), 144.62 (C_{quat}), 152.5 (C_{quat}). IR (ATR): $\tilde{\nu}$ [cm^{-1}] 3044 (w), 2220 (w), 1605 (m), 1495 (s), 1481 (w), 1460 (m), 1435 (w), 1362 (m), 1287 (w), 1082 (w), 1065 (w), 1026 (w), 1005 (w), 970 (m), 955 (w), 918 (w), 820 (s), 766 (w), 735 (w), 692 (s), 667 (w). ESI (*m*/*z* (%)): 398 ([M^+ + H], 1), 397 ([M^+], 4), 309 (49), 308 (100), 232 (13), 105 (12), 77 ([$C_6H_5^+$], 12), 51 ([$C_4H_3^+$], 3). UV/Vis (CH_2Cl_2): λ_{max} [nm] (ε [L cm^{-1} mol^{-1}]) = 257.0 (27 400), 307.5 sh (18 900). Emission (CH_2Cl_2): λ_{max} [nm] (Φ_f) = 387.0 (0.12). Stokes shift [cm^{-1}] = 6700. Anal. calcd for $C_{29}H_{19}N_3$ (397.5): C 84.61, H 4.82, N 10.57; found: C 84.53, H 4.61, N 10.28%.

1-(4-(5-Methylthiophen-2-yl)phenyl)-3,5-diphenyl-1*H*-pyrazole (8d). According to GP3 431 mg (55%) of compound **8d** were obtained as a yellow orange solid; Mp 115 °C. ^{1}H NMR (600 MHz, $CDCl_3$) δ = 2.51 (s, 3H), 6.74 (d, J = 3.5 Hz, 1H), 6.84 (s, 1H), 7.12 (d, J = 3.5 Hz, 1H), 7.39–7.29 (m, 7H), 7.45 (t, J = 7.6 Hz, 3H), 7.53 (d, J = 8.4 Hz, 2H), 7.94 (d, J = 7.9 Hz, 2H). ^{13}C NMR (151 MHz, $CDCl_3$) δ = 15.6 (CH_3), 105.5 (CH), 123.5 (CH), 125.6 (CH), 125.8 (CH), 126.0 (CH), 126.5 (CH), 128.2 (CH), 128.5 (CH), 128.7 (CH), 128.8 (CH), 128.9 (CH), 130.7 (C_{quat}), 133.1 (C_{quat}), 133.9 (C_{quat}), 138.9 (C_{quat}), 140.2 (C_{quat}), 141.0 (C_{quat}), 144.4 (C_{quat}), 152.1 (C_{quat}). IR (ATR): $\tilde{\nu}$ [cm^{-1}] 3065 (w), 2980 (w), 2914 (w), 1545 (w), 1512 (m), 1485 (m), 1460 (m), 1433 (w), 1362 (w), 1261 (w), 1215 (w), 1180 (w), 1163 (w), 1107 (w), 972 (m), 914 (w), 837 (s), 802 (s), 758 (s), 702 (m), 687 (s), 667 (w). GC-MS (*m*/*z* (%)): 392 ([M^+], 1), 330 (20), 297 (22), 296 (100), 295 ([$C_{21}H_{15}N_2^+$], 53), 192 ([$C_{14}H_{14}N_2^+$], 8), 165 ([$C_{13}H_9^+$], 11), 77 ([$C_6H_5^+$], 10), 51 ([$C_4H_3^+$], 4). UV/Vis (CH_2Cl_2): λ_{max} [nm] (ε [L cm^{-1} mol^{-1}]) = 268.5 (29 500). Emission (CH_2Cl_2): λ_{max} [nm] (Φ_f) = 385.0 (0.29). Stokes shift [cm^{-1}] = 11 300. Anal. calcd for $C_{26}H_{20}N_2S$ (392.5): C 79.56, H 5.14, N 7.14; found: C 79.39, H 4.89, N 7.18%.

5-(4-Methoxyphenyl)-1-(4′-methyl-[1,1′-biphenyl]-4-yl)-3-phenyl-1*H*-pyrazole (8e). According to GP3 365 mg (44%) of compound **8e** were obtained as an orange solid; Mp 107 °C. ^{1}H NMR (600 MHz, $CDCl_3$) δ = 2.41 (s, 3H), 3.87 (s, 3H), 6.78 (s, 1H), 6.99 (d, J = 8.8 Hz, 2H), 7.26 (d, J = 7.9 Hz, 2H), 7.35 (br, 5H), 7.43 (d, J = 8.5 Hz, 2H), 7.50 (d, J = 8.1 Hz, 2H), 7.56 (d, J = 8.6 Hz, 2H), 7.88 (d, J = 8.8 Hz, 2H). ^{13}C NMR (151 MHz, $CDCl_3$) δ = 21.2 (CH_3), 55.4 (CH_3), 105.0 (CH), 114.2 (CH), 125.5 (CH), 126.0, 127.0 (CH), 127.2 (CH), 127.4 (CH), 128.4 (CH), 128.6 (CH), 128.9 (CH), 129.7 (CH), 130.9 (C_{quat}), 137.4 (C_{quat}), 137.5 (C_{quat}), 139.2 (C_{quat}), 140.1 (C_{quat}), 144.4 (C_{quat}), 152.0 (C_{quat}), 159.7 (C_{quat}). IR (ATR): $\tilde{\nu}$ [cm^{-1}] 2997 (w), 2917 (w), 1609 (w), 1501 (m), 1485 (m), 1456 (w), 1433 (m), 1358 (w), 1246 (m), 1169 (w), 1111 (w), 1030 (m), 955 (w), 924 (w), 841 (m), 806 (s), 764 (s), 733 (w), 698 (m), 675 (m). ESI (*m*/*z* (%)): 416 ([M^+], 5), 327 (5), 326 ([$C_{22}H_{18}N_2O^+$], 19), 239 (14), 238 (86), 237 (100), 223 (11), 195 (12), 165 ([$C_{13}H_9^+$], 11), 135 (55), 107 ([$C_7H_7O^+$], 11), 103 (13), 92 ([$C_7H_8^+$], 12), 77 ([$C_6H_5^+$], 27), 65 ([$C_5H_5^+$], 3), 51 ([$C_4H_3^+$], 6), 43 (48). UV/Vis (CH_2Cl_2): λ_{max} [nm] (ε [L cm^{-1} mol^{-1}]) = 261.5 (39 900), 288.0 sh (29 600), 311.0 sh (20 500). Emission (CH_2Cl_2): λ_{max} [nm] (Φ_f) = 386.5 (0.37). Stokes shift [cm^{-1}] = 6300. Anal. calcd for $C_{29}H_{24}N_2O$ (416.5): C 83.63, H 5.82, N 6.73; found: C 83.43, H 5.89, N 6.66%.

5-(2-Chlorophenyl)-1-(4′-methyl-[1,1′-biphenyl]-4-yl)-3-phenyl-1*H*-pyrazole (8f). According to GP3 159 mg (19%) of compound **8f** were obtained as a colorless solid; Mp 118 °C. ^{1}H NMR (600 MHz, $CDCl_3$) δ = 2.41 (s, 3H), 6.89 (s, 1H), 7.26 (d, J = 7.5 Hz, 2H), 7.31 (d, J = 7.6 Hz, 1H), 7.37 (m, 4H), 7.41 (d, J = 8.4 Hz, 2H), 7.47 (d, J = 8.7 Hz, 4H), 7.53 (d, J = 7.6 Hz, 2H), 7.99 (d, J = 7.5 Hz, 2H); additional signal for the minor regioisomer: δ = 8.03 (d, J = 7.6 Hz); ratio of regioisomers = 10 : 1. ^{13}C NMR (151 MHz, $CDCl_3$) δ = 21.2 (CH_3), 107.0 (CH), 124.3 (CH), 126.0 (CH), 127.0 (CH), 127.3 (CH), 128.2 (CH), 128.8 (CH), 129.7 (CH), 130.2 (CH), 130.4 (CH), 130.55 (C_{quat}), 132.3 (CH), 133.1 (C_{quat}), 134.2 (C_{quat}), 137.3 (C_{quat}), 137.5 (C_{quat}), 139.2 (C_{quat}), 139.9 (C_{quat}), 141.1 (C_{quat}), 151.9 (C_{quat}); additional signal for the minor regioisomer: δ = 109.3 (CH). IR (ATR): $\tilde{\nu}$ [cm^{-1}] 3022 (w), 2918 (w), 1601 (w), 1503 (s), 1456 (m), 1362 (w), 1124 (w), 1113 (w), 955 (m), 918 (w), 849 (m), 812 (s), 800 (m), 764 (s), 725 (m), 683 (s). ESI (*m*/*z* (%)): 421 ([M^+], 5), 420 (14), 333 (7), 332 (34), 331 (31), 330 (100), 329 (30), 296 (13), 295 (54), 267 (10), 192 ([$C_{14}H_{14}N_2^+$], 17), 165 ([$C_{13}H_9^+$], 16), 147 ([$C_{11}H_{16}^+$], 14), 146 (14), 91 ([$C_7H_7^+$], 5), 77 ([$C_6H_5^+$], 16), 51 ([$C_4H_3^+$], 6). UV/Vis (CH_2Cl_2): λ_{max} [nm] (ε [L cm^{-1} mol^{-1}]) = 256.5 (27 300), 296.0 (28 400). Emission (CH_2Cl_2): λ_{max} [nm] (Φ_f) = 388.5 (0.35). Stokes shift [cm^{-1}] = 8000. HRMS calcd for $C_{28}H_{21}N_2Cl$ + H^+: 421.1472; found: 421.14564.

1-(4′-Methyl-[1,1′-biphenyl]-4-yl)-3-phenyl-5-(thiophen-2-yl)-1*H*-pyrazole (8g). According to GP3 430 mg (55%) of compound **8g** were obtained as an orange solid; Mp 87 °C. ^{1}H NMR (300 MHz, $CDCl_3$) δ = 2.41 (s, 3H), 6.90 (s, 1H), 6.98 (dd, J = 5.1, 3.6 Hz, 1H), 6.92 (dd, J = 3.6, 1.1 Hz, 1H), 7.27 (d, J = 7.9 Hz, 2H), 7.31 (dd, J = 5.1, 1.1 Hz, 1H), 7.36 (d, J = 7.2 Hz, 1H), 7.41–7.46 (m, 3H), 7.56–7.49 (m, 4H), 7.64 (d, J = 8.6 Hz, 2H), 7.93 (d, J = 7.1 Hz, 2H); additional signal for the minor regioisomer: δ = 6.88 (s); ratio of regioisomers = 22 : 1. ^{13}C NMR (75 MHz, $CDCl_3$) δ = 21.3 (CH), 105.2 (CH), 125.9 (CH), 126.4 (CH), 126.7 (CH), 127.07 (CH), 127.50 (CH), 127.54 (CH), 127.57 (CH), 128.2 (CH), 128.8 (CH), 129.7 (CH), 131.5 (C_{quat}), 132.9 (C_{quat}), 137.3 (C_{quat}), 137.7 (C_{quat}), 138.3 (C_{quat}), 138.9 (C_{quat}), 141.2 (C_{quat}), 152.1 (C_{quat}). IR (ATR): $\tilde{\nu}$ [cm^{-1}] 3080 (w), 2945 (w), 1915 (w), 1603 (w), 1499 (s); 1449 (m), 1362 (w), 1283 (w), 1229 (w), 1159 (m), 1115 (w), 1006 (m), 959 (m), 918 (w); 831 (m), 812 (s), 795 (m), 766 (s), 741 (w), 692 (s). GC-MS (m/z (%)): 392 ([M^+], 11), 302 ([$C_{19}H_{14}N_2S^+$], 12), 215 (14), 214 (65), 213 ([$C_{13}H_{11}NS^+$], 100), 185 (24), 111 ([$C_6H_7S^+$], 30), 103 ([$C_8H_7^+$], 13), 77 ([$C_6H_5^+$], 14), 51 ([$C_4H_3^+$], 6). UV/Vis (CH_2Cl_2): λ_{max} [nm] (ε [L cm^{-1} mol^{-1}]) = 272.5 (39 600). Emission (CH_2Cl_2): λ_{max} [nm] (Φ_f) = 394.0 (0.30). Stokes shift [cm^{-1}] = 11 300. Anal. calcd for $C_{26}H_{20}N_2S$ (392.5): C 79.56, H 5.14, N 7.14; found: C 79.41, H 5.35, N 6.91%.

3-Butyl-1-(4′-methyl-[1,1′-biphenyl]-4-yl)-5-phenyl-1*H*-pyrazole (8h). According to GP3 440 mg (60%) of compound **8h** were obtained as a colorless light yellow solid; Mp 64 °C. ^{1}H NMR (300 MHz, $CDCl_3$), 1.00 (t, J = 7.3 Hz, 3H), 1.50 (m, 2H), 1.77 (m, 2H), 2.42 (s, 3H), 2.83–2.71 (m, 3H), 6.36 (s, 1H), 7.26 (d, J = 8.7 Hz, 2H), 7.30–7.39 (m, 7H), 7.50 (d, J = 8.2 Hz, 2H), 7.54 (d, J = 8.7 Hz, 2H); additional signals for the minor regioisomer: δ = 0.94 (t, J = 7.3 Hz), 6.59 (s); ratio of regioisomers = 6 : 1. ^{13}C NMR (75 MHz, $CDCl_3$) δ = 14.1 (CH_3), 21.2 (CH_3), 22.8 (CH_2), 28.2 (CH_2), 32.0 (CH_2), 107.0 (CH), 125.4 (CH), 127.0 (CH), 127.3 (CH), 128.2 (CH), 128.6 (CH), 128.8 (CH), 129.65 (CH), 131.1 (C_{quat}), 137.4 (C_{quat}), 139.3 (C_{quat}), 139.8 (C_{quat}), 143.5 (C_{quat}), 154.5 (C_{quat}); additional signals for the minor regioisomer: δ = 103.0 (CH), 127.1 (CH), 127.7 (CH), 128.7 (CH), 129.74 (CH). IR (ATR): $\tilde{\nu}$ [cm^{-1}] 3032 (w), 2955 (w), 2928 (w), 1605 (w), 1503 (s), 1456 (w), 1423 (w), 1369 (m), 1261 (w), 1192 (w), 1105 (w), 999 (w), 966 (m), 920 (w), 851 (m), 812 (s), 768 (s), 698 (s), 673 (w). GC-MS (m/z (%)): 366 ([M^+], 19), 355 (24), 337 (12), 325 (26), 324 (100), 281 (19), 221 (24), 147 (21), 77 (3). UV/Vis (CH_2Cl_2): λ_{max} [nm] (ε [L cm^{-1} mol^{-1}]) = 286.0 (22 900). Emission (CH_2Cl_2): λ_{max} [nm] (Φ_f) = 382.5 (0.33). Stokes shift [cm^{-1}] = 8800. HRMS calcd for $C_{26}H_{26}N_2$ + H^+: 367.2174; found: 367.2175.

Acknowledgements

Dedicated to Prof. Dr Karl Kleinermanns on the occasion of his 65th birthday. The authors cordially thank the Fonds der Chemischen Industrie for financial support.

Notes and references

1 P. S. Parameswaran, C. G. Naik and V. R. Hegde, *J. Nat. Prod.*, 1997, **60**, 802.
2 K. Motoba, H. Nishizawa, T. Suzuki, H. Hamaguchi, M. Uchida and S. Funayama, *Pestic. Biochem. Physiol.*, 2000, **67**, 73; M. Beckmann and K.-J. Haack, *Chem. Unserer Zeit*, 2003, **37**, 88.
3 R. E. Orth, *J. Pharm. Sci.*, 1968, **57**, 537; A. Chauhan, P. K. Sharma and N. Kaushik, *Int. J. ChemTech Res.*, 2011, **3**, 11; M. A. H. Ismail, J. Lehmann, D. A. Abou El Ella, A. Albohy and K. A. M. Abouzid, *Med. Chem. Res.*, 2009, **18**, 725; S. R. Stauffer, C. J. Coletta, R. Tedesco, G. Nishiguchi, K. Carlson, J. Sun, B. S. Katzenellenbogen and J. A. Katzenellenbogen, *J. Med. Chem.*, 2000, **43**, 4934.
4 R. A. Singer, S. Caron, R. E. McDermott, R. Arpin and N. M. Do, *Synthesis*, 2003, 1727; A. Mukherjee and A. Sarka, *Tetrahedron Lett.*, 2004, **45**, 9525.
5 A. Dorlars, C.-W. Schellhammer and J. Schroeder, *Angew. Chem., Int. Ed.*, 1975, **14**, 665.
6 J. Catalan, F. Fabero, R. M. Claramunt, M. D. Santa Maria, M. de la Concepcion Foces-Foces, F. Hernandez Cano, M. Martinez-Ripoll, J. Elguero and R. Sastre, *J. Am. Chem. Soc.*, 1992, **114**, 5039.
7 Z. Yang, K. Zhang, F. Gong, S. Li, J. Chen, J. Shi Ma, L. N. Sobenina, A. I. Mikhaleva, B. A. Trofimov and G. Yang, *J. Photochem. Photobiol., A*, 2011, **217**, 29.
8 For a recent monograph, see*Organic Light-Emitting Diodes – Synthesis, Properties, and Applications*, ed. K. Müllen and U. Scherf, Wiley-VCH Verlag GmbH & Co. KGaA, Weinheim, 2006.
9 For diversity oriented syntheses of functional π-systems, see (*a*) T. J. J. Müller and D. M. D'Souza, *Pure Appl. Chem.*, 2008, **80**, 609; (*b*) T. J. J. Müller, in *Functional Organic Materials. Syntheses, Strategies, and Applications*, ed. T. J. J. Müller and U. H. F. Bunz, Wiley-VCH Verlag GmbH & Co. KGaA, Weinheim, 2007, p. 179; (*c*) For the concept of diversity oriented synthesis, see *e. g.* M. D. Burke and S. L. Schreiber, *Angew. Chem., Int. Ed.*, 2004, **43**, 46.
10 (*a*) B. Willy and T. J. J. Müller, *Eur. J. Org. Chem.*, 2008, 4157; (*b*) B. Willy and T. J. J. Müller, *Org. Lett.*, 2011, **13**, 2082; (*c*) C. F. Gers, J. Rosellen, E. Merkul and T. J. J. Müller, *Beilstein J. Org. Chem.*, 2011, **7**, 1173; (*d*) L. Levi, C. Boersch, C. F. Gers, E. Merkul and T. J. J. Müller, *Molecules*, 2011, **16**, 9340.
11 I. B. Berlham, *J. Phys. Chem.*, 1970, **74**, 3085.
12 H. S. Im and E. R. Bernstein, *J. Chem. Phys.*, 1988, **88**, 7337.
13 S. A. McFarland and N. S. Finney, *J. Am. Chem. Soc.*, 2001, **123**, 1260.
14 D. M. D'Souza and T. J. J. Müller, *Chem. Soc. Rev.*, 2007, **36**, 1095; N. T. Patil, V. S. Shinde and B. Gajula, *Org. Biomol. Chem.*, 2012, **10**, 211.
15 T. J. J. Müller, *Top. Organomet. Chem.*, 2006, **19**, 149.
16 E. Merkul, C. Boersch, W. Frank and T. J. J. Müller, *Org. Lett.*, 2009, **11**, 2269; A. Zanardi, J. A. Mata and E. Peris, *Organometallics*, 2009, **28**, 4335.
17 J. A. Burkhard, B. Wagner, H. Fischer, F. Schuler, K. Müller and E. M. Carreira, *Angew. Chem., Int. Ed.*, 2010, **49**, 3524.
18 ESI.†
19 F. Vollmer, W. Rettig and E. Birckner, *J. Fluoresc.*, 1994, **4**, 65–69.

20 E. Lippert, *Z. Elektrochem. Ber. Bunsenges. Phys. Chem.*, 1957, **61**, 692; A. Dienes, C. V. Shank and A. M. Trozzolo, Dye Lasers, in *Creation and Detection of the Excited State*, ed. W. R. Ware, Dekker, New York, 1974, vol. 2, p. 149.

21 N. Boens, W. Qin, N. Basarić, J. Hofkens, M. Ameloot, J. Pouget, J.-P. Lefèvre, B. Valeur, E. Gratton, M. van de Ven, N. D. Silva Jr, Y. Engelborghs, K. Willaert, A. Sillen, G. Rumbles, D. Phillips, A. J. W. G. Visser, A. van Hoek, J. R. Lakowicz, H. Malak, I. Gryczynski, A. G. Szabo, D. T. Krajcarski, N. Tamai and A. Miura, *Anal. Chem.*, 2007, **79**, 2137.

22 For determination of fluorescence quantum yields, see *e. g.* S. Fery-Forgues and D. Lavabre, *J. Chem. Educ.*, 1999, **76**, 1260.

23 F. Hirayama, W. Rothman and S. Lipsky, *Chem. Phys. Lett.*, 1970, **5**, 296.

24 M. J. Frisch, G. W. Trucks, H. B. Schlegel, G. E. Scuseria, M. A. Robb, J. R. Cheeseman, G. Scalmani, V. Barone, B. Mennucci, G. A. Petersson, H. Nakatsuji, M. Caricato, X. Li, H. P. Hratchian, A. F. Izmaylov, J. Bloino, G. Zheng, J. L. Sonnenberg, M. Hada, M. Ehara, K. Toyota, R. Fukuda, J. Hasegawa, M. Ishida, T. Nakajima, Y. Honda, O. Kitao, H. Nakai, T. Vreven, J. A. Montgomery Jr, J. E. Peralta, F. Ogliaro, M. Bearpark, J. J. Heyd, E. Brothers, K. N. Kudin, V. N. Staroverov, R. Kobayashi, J. Normand, K. Raghavachari, A. Rendell, J. C. Burant, S. S. Iyengar, J. Tomasi, M. Cossi, N. Rega, J. M. Millam, M. Klene, J. E. Knox, J. B. Cross, V. Bakken, C. Adamo, J. Jaramillo, R. Gomperts, R. E. Stratmann, O. Yazyev, A. J. Austin, R. Cammi, C. Pomelli, J. W. Ochterski, R. L. Martin, K. Morokuma, V. G. Zakrzewski, G. A. Voth, P. Salvador, J. J. Dannenberg, S. Dapprich, A. D. Daniels, O. Farkas, J. B. Foresman, J. V. Ortiz, J. Cioslowski and D. J. Fox, *GAUSSIAN 09 (Revision A.02)*, Gaussian, Inc., Wallingford CT, 2009.

25 C. Lee, W. Yang and R. G. Parr, *Phys. Rev. B: Condens. Matter Mater. Phys.*, 1988, **37**, 785; A. D. Becke, *J. Chem. Phys.*, 1993, **98**, 1372; A. D. Becke, *J. Chem. Phys.*, 1993, **98**, 5648; K. Kim and K. D. Jordan, *J. Phys. Chem.*, 1994, **98**, 10089; P. J. Stephens, F. J. Devlin, C. F. Chabalowski and M. J. Frisch, *J. Phys. Chem.*, 1994, **98**, 11623.

26 R. Krishnan, J. S. Binkley, R. Seeger and J. A. Pople, *J. Chem. Phys.*, 1980, **72**, 650.

27 G. Scalmani and M. J. Frisch, *J. Chem. Phys.*, 2010, **132**, 114110.

28 H.-S. Im and E. R. Bernstein, *J. Chem. Phys.*, 1988, **88**, 7337.

29 T. Yanai, D. Tew and N. Handy, *Chem. Phys. Lett.*, 2004, **393**, 51.

30 A. M. Berezhkovskii, *Chem. Phys.*, 1992, **164**, 331; R. Cammi and J. Thomasi, *Int. J. Quantum Chem., Quantum Chem. Symp.*, 1995, **29**, 465; B. Mennucci, R. Cammi and J. Tomasi, *J. Chem. Phys.*, 1998, **109**, 2798; X.-Y. Li and K.-X. Fu, *J. Comput. Chem.*, 2004, **25**, 500; R. Cammi, S. Corni, B. Mennucci and J. Tomasi, *J. Chem. Phys.*, 2005, **122**, 104513.

31 Density functional theory for excited states: equilibrium structure and electronic spectra. F. Furche and D. Rappoport, ch. III of "Computational Photochemistry", M. Olivucci, ed., vol. 16 of "Computational and Theoretical Chemistry", Elsevier, Amsterdam, 2005.

32 TURBOMOLE V6.3 2013, a development of University of Karlsruhe and Forschungszentrum Karlsruhe GmbH, 1989–2007, TURBOMOLE GmbH, since 2007, available from http://www.turbomole.com.

33 Electronic Structure Calculations on Workstation Computers: The Program System TURBOMOLE. R. Ahlrichs, M. Bär, M. Häser, H. Horn and C. Kölmel, *Chem. Phys. Lett.*, 1989, **162**, 165.

34 A. Schäfer, C. Huber and R. Ahlrichs, *J. Chem. Phys.*, 1994, **100**, 5829.

35 A. Klamt and G. Schüürmann, *J. Chem. Soc., Perkin Trans. 2*, 1993, 799.

36 F. Furche and R. Ahlrichs, *J. Chem. Phys.*, 2002, **117**, 7433.

